行政院國家科學委員會專題研究計畫　成果報告

多輸入多輸出有限脈衝系統的盲判別與對等化(3/3)

計畫類別：個別型計畫
計畫編號：NSC94-2213-E-009-010-
執行期間：94 年 08 月 01 日至 95 年 07 月 31 日
執行單位：國立交通大學電機與控制工程學系(所)

計畫主持人：林清安

計畫參與人員：陳益生

報告類型：完整報告
報告附件：出席國際會議研究心得報告及發表論文
處理方式：本計畫可公開查詢

中　華　民　國 95 年 10 月 11 日

行政院國家科學委員會補助專題研究計畫　成果報告

多輸入多輸出有限脈衝系統的盲判別與對等化

計畫類別：個別型計畫

計畫編號：NSC92－2213－E－009－085
NSC93－2213－E－009－041
NSC94－2213－E－009－010

執行期間：92 年 8 月 1 日至 95 年 7 月 31 日

計畫主持人：林清安
計畫參與人員：陳益生

成果報告類型：完整報告
成果報告附件：出席國際學術會議心得報告及發表之論文(三年三份)
處理方式：本計畫可公開查詢

執行單位：國立交通大學電機與控制工程學系(所)

中　華　民　國　95　年　10　月　5　日

多輸入多輸出有限脈衝系統的盲判別與對等化

中文摘要

本報告針對多出入多輸出頻率選擇衰減之無線通信系統提出了三種通道盲蔽判別的方法。判別的方法是利用所估測出來的接收信號協方差矩陣, 先計算出通道乘積矩陣, 再對此通道乘積矩陣取特徵分解, 即可求出通道脈衝響應矩陣。所提出的方法都是利用對傳送信號作不同的編碼方式所引發的循環穩態特性來求解問題。我們分別考慮了以下三種不同的編碼方式: (1) 週期性編碼, (2) 週期性編碼加補零, (3) 補零。對前兩種判別方法, 我們也設計了最佳的週期性編碼器。我們的方法在正規均方差的表現上可與子空間的方法相比, 但只需要較少的計算量, 同時判別條件也較爲寬鬆, 另外我們的方法還可適用於發射器數目較接收器數目多或者少的情況。數值模擬的結果顯示我們所提出的方法對通道階數過估的情況具有相當的強健性。

關鍵詞: 多出入多輸出通道, 盲蔽判別, 週期性編碼, 有限脈衝響應, 補零, 單載波補零傳輸系統, 正交分頻多工系統。

Blind Identification and Equalization for Multiple-input Multiple-output Finite Impulse Systems

Abstract

We propose three blind identification algorithms for multiple-input multiple-output (MIMO) frequency selective fading wireless communication channels. The algorithms compute the channel product matrices from the estimated covariance matrix of the received data and then determine the channel impulse response matrix via an eigenvalue-eigenvector decomposition. The algorithms are all based on transmitter-induced cyclostationarity through precoding. Three precoding are considered: (i) periodic precoding, (ii) periodic precoding plus zero padding, and (iii) zero padding alone. The algorithms, with optimally designed periodic precoding, have normalized root-mean-squared error (NRMSE) performance comparable with subspace methods but require less computation, allow a more relaxed identifiability condition, and are applicable to general MIMO systems with more transmitters or more receivers. Simulation results show that the algorithms are reasonably robust with respect to channel order overestimation.

Key words: MIMO channels, blind identification, periodic precoding (modulation), finite impulse response, zero padding, single carrier zero padding transmission systems, OFDM systems

Contents

Chapter 1

Introduction

1.1 Research Objective

Multiple-input multiple-output (MIMO) communication systems employing multiple transmit and receive antennas have received much attention due to the potential improvement in data transmission rate and link reliability they can offer. However, to exploit the potential advantage of MIMO systems, accurate channel state information is required. Channel can be identified or estimated using training signal which requires additional bandwidth. As a means to eschewing the need of training signal and the associated bandwidth requirement, blind identification of MIMO channels has been the focus of much research. Many blind identification algorithms have been proposed in recent years (see [1, 2] for a detailed review).

Existing algorithms for blind identification of MIMO finite impulse response (FIR) channels can be classified into second-order statistics methods [8]-[12],[20]-[22], higher-order statistics methods [3]-[5], and deterministic methods [6, 7]. Among these three types of methods, blind identification based on second-order statistics has been widely studied because it requires fewer data samples than the high-order statistics approach and it avoids poor estimation accuracy under low SNR, a common shortcoming of deterministic methods. Existing second-order statistics methods for MIMO systems, e.g., the subspace methods [8, 9], [26], [28]-[29], the linear prediction methods [10]-[12], and the matrix outer product decomposition methods [20]-[22], either impose restrictive assumptions on the channel to be identified or require large amount of computations, that may not be realistic in practical applications.

The goal of this research is to develop blind identification algorithms for MIMO channels,

that are simple in computation and less restrictive in assumptions. It is hoped that the algorithms developed are thus more practical from an application point of view.

1.2 Literature Survey

It is well-known that cyclostationarity of the received data is the key to all blind identification based on second-order statistics [1, 2]. Cycloststionarity can be induced either at the receiver, by oversampling or multiple antennas, or at the transmitter, by various coding methods. An advantage of transmitter-induced cyclostationarity is that the resulting identification methods require less restrictive assumption on the channel, for example, channels with nonminimum phase zeros can be handled. One effective way to induce cyclostationarity at the transmitter is by periodic precoding. Blind identification methods for general MIMO FIR channels using periodic precoding are found in [17, 18]. In [17], Chevreuil and Loubaton proposes a scheme that multiplies the input sequence by a constant modulus complex exponential precoding sequence to induce conjugate cyclostationarity at the transmitter. The scheme reduces the MIMO channel identification problem to several SIMO ones, which are then solved by the subspace method [24]. Each SIMO channel is required to be free from common zeros. However, the method in [17] allows only real input symbols and the identifiability condition is irreducible and column reduced. Bölcskei et. al. [18] proposes a method for identifying each of the scalar channels individually up to a phase ambiguity using non-constant modulus periodic precoding sequences. The method imposes no restriction on channel zeros and is insensitivity to channel order overestimation. However, no systematic procedure for the design of the precoding sequences is given. In this report, we propose an identification method based on periodic precoding, which allows complex input symbols and gives an optimal design of the precoding sequence.

Single carrier zero padding (SC-ZP) block transmission systems, another communication systems, are used to remove interblock interference (IBI) [13, 14, 25, 26]. In the literature, to the best of our knowledge, there is only one paper, by Zeng and Ng [26], that proposes a subspace method for blind identification of MIMO SC-ZP block transmission systems. The method can be used to identify the channel impulse response matrix up to a matrix ambiguity when the channel is irreducible and the channel noise is uncorrelated and white. In this report, we first propose an identification method for MIMO SC-ZP systems based on periodic precoding, which can further relax the identifiability condition and reduce the computational load, compared with the method in [26]. In addition, we also propose another simplified identification method for such systems without periodic precoding. This simplified method can also apply to MIMO zero padding orthogonal frequency division multiplexing (ZP-OFDM) systems.

1.3 Organization of the Report

The report is organized as follows. In Chapter 2, we propose a blind identification method for general MIMO FIR channels based on periodic precoding. We also discuss the optimal design of the precoding sequence which takes into account the effect of additive channel noise and numerical error. We also propose a blind identification method for MIMO FIR channels in SC-ZP block transmission systems based on periodic precoding and discuss the optimal design of the precoding sequence in Chapter 3. In Chapter 4, we first propose a blind identification for SC-ZP block transmission systems without periodic precoding. Extension of this method to ZP-OFDM systems is given subsequently. Chapter 5 concludes this report and discusses the related future research.

We define the following operations that will be used in the derivation of the main result. First, for any $m \times m$ matrix $\mathbf{A} = [a_{k,l}]_{0 \le k,l \le m-1}$, define $\Gamma_j(\mathbf{A}) = [a_{0,j} \;\; a_{1,j+1} \;\; \cdots \;\; a_{m-1-j,m-1}]^T$ for $0 \le j \le m-1$, i.e., $\Gamma_j(\mathbf{A})$ is the vector formed from the jth super-diagonal of $\mathbf{A}$. Second, for any $Jn \times Jn$ matrix $\mathbf{B} = [\mathbf{B}_{k,l}]_{0 \le k,l \le n-1}$, where $\mathbf{B}_{k,l}$ is a block matrix of dimension $J \times J$, define $\Upsilon_j(\mathbf{B}) = [\mathbf{B}_{0,j}^T \;\; \mathbf{B}_{1,j+1}^T \;\; \cdots \;\; \mathbf{B}_{n-1-j,n-1}^T]^T$ for $0 \le j \le n-1$, i.e., $\Upsilon_j(\mathbf{B})$ is the matrix formed from the jth block super-diagonal of $\mathbf{B}$.

Chapter 2

Identification of General MIMO Channels

In this chapter, we propose a blind identification method for MIMO FIR channels based on periodic precoding. It is shown that, by properly choosing the precoding sequence, the MIMO FIR transfer functions, with K inputs and J outputs, can be identified up to a unitary matrix ambiguity. The transfer functions need not be irreducible or column reduced, and there can be more outputs ($J \geq K$) or more inputs ($J < K$). The method exploits the linear relation between the covariance matrix of the received data and the "channel product matrices". The method is shown to be robust with respect to channel order overestimation. The proposed algorithm requires solving linear equations and computing the nonzero eigenvalues and eigenvectors of a Hermitian positive semidefinite matrix. The performance of the algorithm, and indeed the identifiability, depends on the choice of the precoding sequence. We propose a method for optimal selection of the precoding sequence which takes into account the effect of additive channel noise and numerical error in covariance matrix estimation. Simulation results are used to demonstrate the performance of the algorithm.

2.1 System Model and Formulation

We consider the linear MIMO baseband model of a communication channel with K transmitters and J receivers shown in Figure 2.1, where each source symbol sequence is multiplied by a P-periodic sequence, $p(n)$, before transmission. The transmitted signal is

$$w_k(n) = p(n)s_k(n), \quad k = 1, 2, \cdots, K, \tag{2.1}$$

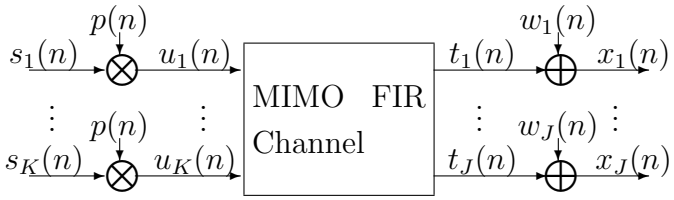

Figure 2.1. An MIMO channel model

where $p(n+P) = p(n)$, $\forall\, n$. The discrete time model describing the relation between the transmitted signal $u_k(n)$ and the received signal $x_j(n)$ has the form of an MIMO FIR filter with additive noise:

$$x_j(n) = \sum_{k=1}^{K} \sum_{l=0}^{L_{jk}} h_{jk}(l) u_k(n-l) + w_j(n), \quad j = 1, 2, \cdots, J, \tag{2.2}$$

where $h_{jk}(0)$, $h_{jk}(1)$, $\cdots$, $h_{jk}(L_{jk})$, are the impulse responses of the channel between the kth transmitter and the jth receiver, and $w_j(n)$ is the channel noise seen at the input of the jth receiver. The equations (2.1) and (2.2) can be written more compactly as

$$\mathbf{u}(n) = p(n)\mathbf{s}(n), \quad \mathbf{x}(n) = \sum_{l=0}^{L} \mathbf{H}(l)\mathbf{u}(n-l) + \mathbf{w}(n), \tag{2.3}$$

where $\mathbf{u}(n)$, $\mathbf{s}(n) \in \mathbb{C}^K$, and $\mathbf{x}(n)$, $\mathbf{w}(n) \in \mathbb{C}^J$ are vector signals formed by stacking the respective scalar signals together, e.g., $\mathbf{x}(n) = [x_1(n)\ \ x_2(n)\ \ \cdots\ \ x_J(n)]^T$. The jkth element of $\mathbf{H}(l) \in \mathbb{C}^{J\times K}$ is $h_{jk}(l)$, and $L = \max_{j,k}\{L_{jk}\}$ is the order of the MIMO channel. Thus $\mathbf{H}(L) \neq \mathbf{0}_{J\times K}$.

Group the sequence of $\mathbf{x}(n)$ as $\bar{\mathbf{x}}(n) = [\mathbf{x}(Pn)^T, \mathbf{x}(Pn+1)^T, \cdots, \mathbf{x}(Pn+P-1)^T]^T \in \mathbb{C}^{KP}$, and let $\bar{\mathbf{w}}(n), \bar{\mathbf{u}}(n), \bar{\mathbf{s}}(n)$ be similarly defined, we have

$$\bar{\mathbf{x}}(n) = \mathbf{H_0}\bar{\mathbf{u}}(n) + \mathbf{H_1}\bar{\mathbf{u}}(n-1) + \bar{\mathbf{w}}(n), \tag{2.4}$$

where $\mathbf{H_0}$ is an $JP \times KP$ block lower-triangular Toeplitz matrix with $[\mathbf{H}(0)^T\ \mathbf{H}(1)^T \cdots \mathbf{H}(L)^T\ \mathbf{0}_{J\times K}^T \cdots \mathbf{0}_{J\times K}^T]^T \in \mathbb{C}^{JP\times K}$ as its first block column (i.e., the first K columns), and $\mathbf{H_1}$ is an $JP \times KP$ block upper-triangular Toeplitz matrix with $[\mathbf{0}_{J\times K} \cdots \mathbf{0}_{J\times K}\ \mathbf{H}(L)\ \mathbf{H}(L-1) \cdots \mathbf{H}(1)] \in \mathbb{C}^{J\times KP}$ as its first block row (i.e., the first J rows). Since $p(n)$ is periodic, $\bar{\mathbf{u}}(n) = \mathbf{G}\bar{\mathbf{s}}(n)$ for all n, where $\mathbf{G} = \mathrm{diag}[p(0)\mathbf{I}_K, p(1)\mathbf{I}_K, \cdots, p(P-1)\mathbf{I}_K] \in \mathbb{R}^{KP\times KP}$ is a diagonal matrix, (2.4) can be written as

$$\bar{\mathbf{x}}(n) = \mathbf{H_0}\mathbf{G}\bar{\mathbf{s}}(n) + \mathbf{H_1}\mathbf{G}\bar{\mathbf{s}}(n-1) + \bar{\mathbf{w}}(n), \tag{2.5}$$

We assume that the receivers are synchronized with the transmitters. In addition, the following assumptions are made throughout this chapter.

(A1) $\mathbf{s}(n)$ and $\mathbf{w}(n)$ are white zero-mean vector sequences, and $\mathbf{s}(n)$ and $\mathbf{w}(n)$ are temporally and spatially uncorrelated. More precisely, $E[\mathbf{s}(k)\mathbf{s}(j)^*] = \delta(k-j)\mathbf{I}_K \in \mathbb{R}^{K\times K}$, $E[\mathbf{w}(k)\mathbf{w}(j)^*] = \delta(k-j)\sigma_w^2\mathbf{I}_J \in \mathbb{R}^{J\times J}$, $E[\mathbf{s}(k)\mathbf{w}(j)^*] = \mathbf{0}_{K\times J}$, $\forall\, k, j$, where $\delta(\cdot)$ is the Kronecker delta function.

(A2) An upper bound $\hat{L}$ of the channel order L is known and the period $P > \hat{L} + 1$.

(A3) The channel impulse response matrix $\mathbf{H} = [\mathbf{H}(0)^T\ \mathbf{H}(1)^T\ \cdots\ \mathbf{H}(L)^T]^T$ is full column rank, i.e., rank($\mathbf{H}$)=K.

In the next section, we will derive an algorithm for blind identification of the MIMO channel impulse response matrix $\mathbf{H}$ using second-order statistics of the received data.

2.2 Blind Channel Identification

In this section, we derive the proposed method for the case under assumptions (**A1**), (**A2**), (**A3**) and noiseless case. We show that by appropriately selecting the periodic precoding sequence, any MIMO channel satisfying (**A3**) is identifiable up to an $K \times K$ unitary matrix ambiguity. The effect of noise and optimal design of the precoding sequence are discussed in Section 2.3.

2.2.1 The Identification Method

We first derive the proposed method for the case where the channel order L is known with $P > L + 1$, there are more receivers, i.e., $J \geq K$, and the noise is absent. We discuss the cases of channel order overestimation and more transmitters than receivers (i.e., $K > J$) in Section 2.2.2 and 2.2.3, respectively.

From (2.5) and assumption (**A1**), the covariance matrix of $\bar{\mathbf{x}}(n)$ can be written as (noiseless case)

$$\mathbf{R}_{\bar{\mathbf{x}}} = E[\bar{\mathbf{x}}(n)\bar{\mathbf{x}}(n)^*] = \mathbf{H_0}\mathbf{G}^2\mathbf{H_0}^* + \mathbf{H_1}\mathbf{G}^2\mathbf{H_1}^*. \tag{2.6}$$

Let $\mathbf{J} \in \mathbb{R}^{P\times P}$ be the matrix whose first sub-diagonal are all one, i.e., $\Gamma_1(\mathbf{J}^T) = [1\ 1\ \cdots\ 1]^T \in \mathbb{R}^{(P-1)}$, and all remaining entries are zero. The block Toeplitz structures of $\mathbf{H_0}$ and $\mathbf{H_1}$ allow us to write $\mathbf{H_0} = \sum_{k=0}^{L} \mathbf{J}^k \otimes \mathbf{H}(k)$ and $\mathbf{H_1} = \sum_{k=0}^{L} (\mathbf{J}^T)^{P-k} \otimes \mathbf{H}(k)$, respectively. Besides, we define $\mathbf{G_p} = \text{diag}[p(0), p(1), \cdots, p(P-1)] \in \mathbb{R}^{P\times P}$. Hence $\mathbf{H_0}\mathbf{G}^2\mathbf{H_0}^*$ can be

written as

$$\begin{aligned}\mathbf{H_0G^2H_0^*} &= \textstyle\sum_{k=0}^{L}\mathbf{J}^k\otimes\mathbf{H}(k)\left(\mathbf{G_p^2}\otimes\mathbf{I}_{M_t}\right)\sum_{l=0}^{L}\left(\mathbf{J}^l\otimes\mathbf{H}(l)\right)^* \\ &= \textstyle\sum_{k=0}^{L}\sum_{l=0}^{L}\left(\mathbf{J}^k\otimes\mathbf{H}(k)\right)\left(\mathbf{G_p^2}\otimes\mathbf{I}_{M_t}\right)\left((\mathbf{J}^T)^l\otimes\mathbf{H}(l)^*\right) \\ &= \textstyle\sum_{k=0}^{L}\sum_{l=0}^{L}\left(\mathbf{J}^k\mathbf{G_p^2}(\mathbf{J}^T)^l\right)\otimes\left(\mathbf{H}(k)\mathbf{H}(l)^*\right),\end{aligned} \tag{2.7}$$

where we have used the identies $(\mathbf{A}\otimes\mathbf{B})^* = \mathbf{A}^*\otimes\mathbf{B}^*$ and $(\mathbf{A}\otimes\mathbf{B})(\mathbf{C}\otimes\mathbf{D}) = (\mathbf{AC})\otimes(\mathbf{BD})$ [35, p.190]. Similarly, $\mathbf{H_1G^2H_1^*}$ can be written as

$$\mathbf{H_1G^2H_1^*} = \sum_{k=0}^{L}\sum_{l=0}^{L}\left((\mathbf{J}^T)^{P-k}\mathbf{G_p^2}\mathbf{J}^{P-l}\right)\otimes\left(\mathbf{H}(k)\mathbf{H}(l)^*\right). \tag{2.8}$$

The following proposition shows that the matrices $\mathbf{J}^k\mathbf{G_p^2}(\mathbf{J}^T)^l$ and $(\mathbf{J}^T)^{P-k}\mathbf{G_p^2}\mathbf{J}^{P-l}$ have special structures that allow decomposition of (2.6) into a group of decoupled equations. Roughly speaking, the jth block super-diagonal part of (2.6) involves only the unknown "channel product matrices", $\mathbf{H}(k)\mathbf{H}(k+j)^*$, $k = 0, 1, \cdots, L-j$. For example, the equations corresponding to the diagonal blocks ($j = 0$) involve only $\mathbf{H}(k)\mathbf{H}(k)^*$, $k = 0, 1, \cdots, L$. In the proposed identification algorithm, these "channel product matrices" are computed first by solving linear equations, and then the channel impulse response matrices $\mathbf{H}(k)$ are computed via eigenvalue-eigenvector decomposition.

Proposition 2.1 : Let $0 \le k, l \le L$ be two non-negative integers. Then

(a) For $l = k + j$, where $0 \le j \le L - k$, both $\mathbf{J}^k\mathbf{G_p^2}(\mathbf{J}^T)^l$ and $(\mathbf{J}^T)^{P-k}\mathbf{G_p^2}\mathbf{J}^{P-l}$ are upper triangular matrices with only the respective jth upper diagonals nonzero, and

$$\Gamma_j\left(\mathbf{J}^k\mathbf{G_p^2}(\mathbf{J}^T)^l\right) = [\underbrace{0\ \cdots\ 0}_{k\ entries}\ \underbrace{p(0)^2\ \ p(1)^2\ \ \cdots\ \ p(P-1-k-j)^2}_{P-k-j\ entries}]^T, \tag{2.9}$$

$$\Gamma_j\left((\mathbf{J}^T)^{P-k}\mathbf{G_p^2}\mathbf{J}^{P-l}\right) = [\underbrace{p(P-k)^2\ \ p(P-k+1)^2\ \ \cdots\ \ p(P-1)^2}_{k\ entries}\ \underbrace{0\ \cdots\ 0}_{P-k-j\ entries}\ ]^T. \tag{2.10}$$

(b) For $l < k$, both $\Gamma_j\left(\mathbf{J}^k\mathbf{G_p^2}(\mathbf{J}^T)^l\right)$ and $\Gamma_j\left((\mathbf{J}^T)^{P-k}\mathbf{G_p^2}\mathbf{J}^{P-l}\right)$ are lower triangular with zero diagonal matrices.

Proof : See [16].

It follows from (2.9) and (2.10) that

$$\begin{aligned}&\Gamma_j\left(\mathbf{J}^k\mathbf{G_p^2}(\mathbf{J}^T)^l\right) + \Gamma_j\left((\mathbf{J}^T)^{P-k}\mathbf{G_p^2}\mathbf{J}^{P-l}\right) \\ &= \begin{cases} [\underbrace{p(P-k)^2\ \cdots\ p(P-1)^2}_{k\ entries}\ \underbrace{p(0)^2\ \cdots\ p(P-1-k-j)^2}_{P-k-j\ entries}]^T & \text{if} \quad j = l-k \ge 0 \\ \mathbf{0}_{(P-j)\times 1} \qquad \text{if} \quad j \ne l-k \end{cases}.\end{aligned} \tag{2.11}$$

Since

$$\Upsilon_j\left(\left(\mathbf{J}^k\mathbf{G}_{\mathbf{p}}^2(\mathbf{J}^T)^l\right)\otimes\mathbf{H}(k)\mathbf{H}(l)^*\right)=\Gamma_j\left(\mathbf{J}^k\mathbf{G}_{\mathbf{p}}^2(\mathbf{J}^T)^l\right)\otimes\mathbf{H}(k)\mathbf{H}(l)^* \tag{2.12}$$

and

$$\Upsilon_j\left(\left((\mathbf{J}^T)^{P-k}\mathbf{G}_{\mathbf{p}}^2\mathbf{J}^{P-l}\right)\otimes\mathbf{H}(k)\mathbf{H}(l)^*\right)=\Gamma_j\left((\mathbf{J}^T)^{P-k}\mathbf{G}_{\mathbf{p}}^2\mathbf{J}^{P-l}\right)\otimes\mathbf{H}(k)\mathbf{H}(l)^*, \tag{2.13}$$

it follows from (2.6)-(2.8) and (2.11)-(2.13) that $\Upsilon_j\left(\mathbf{R}_{\bar{\mathbf{x}}}\right)$ can be derived as follows.

$$\begin{aligned}
&\Upsilon_j\left(\mathbf{R}_{\bar{\mathbf{x}}}\right)\\
&=\Upsilon_j\left(\mathbf{H_0}\mathbf{G}^2\mathbf{H_0^*}+\mathbf{H_1}\mathbf{G}^2\mathbf{H_1^*}\right)\\
&=\textstyle\sum_{k=0}^{L}\sum_{l=0}^{L}\Upsilon_j\left(\left(\mathbf{J}^k\mathbf{G}_{\mathbf{p}}^2(\mathbf{J}^T)^l\right)\otimes\left(\mathbf{H}(k)\mathbf{H}(l)^*\right)\right)+\Upsilon_j\left(\left((\mathbf{J}^T)^{P-k}\mathbf{G}_{\mathbf{p}}^2\mathbf{J}^{P-l}\right)\otimes\left(\mathbf{H}(k)\mathbf{H}(l)^*\right)\right)\\
&=\textstyle\sum_{k=0}^{L}\sum_{l=0}^{L}\{\Gamma_j\left(\mathbf{J}^k\mathbf{G}_{\mathbf{p}}^2(\mathbf{J}^T)^l\right)+\Gamma_j\left((\mathbf{J}^T)^{P-k}\mathbf{G}_{\mathbf{p}}^2\mathbf{J}^{P-l}\right)\}\otimes\mathbf{H}(k)\mathbf{H}(l)^*\\
&=\textstyle\sum_{k=0}^{L-j}[p(P-k)^2\ \cdots\ p(P-1)^2\ p(0)^2\ \cdots\ p(P-1-k-j)^2]^T\otimes\mathbf{H}(k)\mathbf{H}(k+j)^*\\
&=\textstyle\sum_{k=0}^{L-j}[p(P-k)^2\mathbf{I}_J\ \cdots\ p(P-1)^2\mathbf{I}_J\ p(0)^2\mathbf{I}_J\ \cdots\ p(P-1-k-j)^2\mathbf{I}_J]^T\mathbf{H}(k)\mathbf{H}(k+j)^*
\end{aligned} \tag{2.14}$$

The right hand side of (2.14) is a linear combination of block columns with the channel product matrices, $\mathbf{H}(k)\mathbf{H}(k+j)^*$, as coefficients. If we define, for $0\le j\le L$,

$$\mathbf{F}_j=[(\mathbf{H}(0)\mathbf{H}(j)^*)^T\ (\mathbf{H}(1)\mathbf{H}(j+1)^*)^T\ \cdots\ (\mathbf{H}(L-j)\mathbf{H}(L)^*)^T]^T\in\mathbb{C}^{J(L-j+1)\times J}, \tag{2.15}$$

then (2.14) can be written in a more compact form as

$$\Upsilon_j\left(\mathbf{R}_{\bar{\mathbf{x}}}\right)=\mathbf{M}_j\mathbf{F}_j\qquad\forall\ 0\le j\le L, \tag{2.16}$$

where $\mathbf{M}_j\in\mathbb{R}^{J(P-j)\times J(L-j+1)}$ is defined as

$$\mathbf{M}_j=\begin{bmatrix}
p(0)^2 & p(P-1)^2 & p(P-2)^2 & \cdots & p(P-L+j)^2\\
p(1)^2 & p(0)^2 & p(P-1)^2 & \cdots & p(P-L+j+1)^2\\
p(2)^2 & p(1)^2 & p(0)^2 & \cdots & p(P-L+j+2)^2\\
\vdots & \vdots & \vdots & \vdots & \vdots\\
p(P-3-j)^2 & p(P-4-j)^2 & p(P-5-j)^2 & \cdots & p(P-L-3)^2\\
p(P-2-j)^2 & p(P-3-j)^2 & p(P-4-j)^2 & \cdots & p(P-L-2)^2\\
p(P-1-j)^2 & p(P-2-j)^2 & p(P-3-j)^2 & \cdots & p(P-L-1)^2
\end{bmatrix}\otimes\mathbf{I}_J. \tag{2.17}$$

We note that $\mathbf{M}_j$, $1\le j\le L$, is obtained from $\mathbf{M}_0$ by deleting its last jJ rows and last jJ columns.

Since $P>L+1$, the $(L+1)$ equations in (2.16) are overdetermined and for the noise free case, these equations are consistent. We note that the matrix $\mathbf{M}_j$, $j=0,1,\cdots,L$, is completely determined by the precoding sequence. By appropriately selecting the precoding

sequence, we can make each $\mathbf{M}_j$ full column rank. Then the solution $\mathbf{F}_j$ can be obtained as

$$\mathbf{F}_j = (\mathbf{M}_j^T \mathbf{M}_j)^{-1} \mathbf{M}_j^T \Upsilon_j (\mathbf{R}_{\bar{\mathbf{x}}}) . \tag{2.18}$$

If $\mathbf{F}_j$, $0 \leq j \leq L$, are computed from (2.18), then we have the channel product matrices $\mathbf{H}(k)\mathbf{H}(l)^*$ for $0 \leq k \leq l \leq L$. We now consider the computation required to determine the channel impulse response matrix $\mathbf{H}$ from $\mathbf{F}_j$.

Let $\mathbf{Q}$ be the Hermitian matrix defined by $\Upsilon_j(\mathbf{Q}) = \mathbf{F}_j$ for $j = 0, 1, \cdots, L$, and let the channel impulse response matrix $\mathbf{H} = [\mathbf{H}(0)^T \ \mathbf{H}(1)^T \ \cdots \ \mathbf{H}(L)^T]^T$. Clearly we have

$$\mathbf{Q} = \mathbf{H}\mathbf{H}^*. \tag{2.19}$$

Since rank$(\mathbf{H}) = K$ by assumption (**A3**), $\mathbf{Q}$ has rank K. Since $\mathbf{Q}$ is Hermitian and positive semidefinite, $\mathbf{Q}$ has K positive eigenvalues, say, $\lambda_1, \cdots, \lambda_K$. We can expand $\mathbf{Q}$ as

$$\mathbf{Q} = \sum_{j=1}^{K} (\sqrt{\lambda_j}\mathbf{d}_j)(\sqrt{\lambda_j}\mathbf{d}_j)^*, \tag{2.20}$$

where $\mathbf{d}_j$ is a unit norm eigenvector of $\mathbf{Q}$ associated with $\lambda_j > 0$. We can thus choose the channel impulse response matrix to be

$$\widehat{\mathbf{H}} = [\sqrt{\lambda_1}\mathbf{d}_1 \ \sqrt{\lambda_2}\mathbf{d}_2 \ \cdots \ \sqrt{\lambda_K}\mathbf{d}_K] \in \mathbb{C}^{J(L+1)\times K}. \tag{2.21}$$

We note $\mathbf{H}$ can only be identified up to a unitary matrix ambiguity $\mathbf{U} \in \mathbb{C}^{K\times K}$ [20, 21], i.e., $\widehat{\mathbf{H}} = \mathbf{H}\mathbf{U}$, since $\widehat{\mathbf{H}}\widehat{\mathbf{H}}^* = \mathbf{H}\mathbf{H}^* = \mathbf{Q}$. The ambiguity matrix $\mathbf{U}$ is intrinsic to methods for blind identification of multiple input systems using only second-order statistics [20, 21].

2.2.2 Channel Order Overestimation

So far we have assumed that the channel order L is known. If only an upper bound $\hat{L} \geq L$ is available with $P > \hat{L} + 1$, then following the same process given in Section 2.2.1, the corresponding $J(\hat{L}+1) \times J(\hat{L}+1)$ matrix $\mathbf{Q}$ can be similarly constructed as in (2.19). The last $(\hat{L}-L)$ block columns (i.e., $(\hat{L}-L)J$ columns) of $\mathbf{Q}$ are zero, so are its last $(\hat{L}-L)$ block rows. Hence again, $\mathbf{Q}$ is of rank K and has K positive eigenvalues with the associated eigenvectors all of the form $\hat{\mathbf{d}} = [\mathbf{d}^T \ 0 \ \cdots \ 0]^T \in \mathbb{C}^{J(\hat{L}+1)}$ where $\mathbf{d} \in \mathbb{C}^{J(L+1)}$. Thus, we can determine the channel impulse response matrix, up to a unitary matrix ambiguity, from the K eigenvectors associated with the K positive eigenvalues of $\mathbf{Q}$. In the noise free case, we can, in theory, also determine the actual channel order.

2.2.3 More Transmitters Than Receivers

In the above discussions, we assume that there are more receivers than transmitters, i.e., $J \geq K$. If there are more transmitters, i.e., $K > J$, then either $J(L+1) \geq K$ or $K > J(L+1)$. If $J(L+1) \geq K$, then $\mathbf{H}$ is a tall matrix and assumption (**A3**) is generically satisfied [33]. Hence the proposed method still applies. If $K > J(L+1)$, then rank($\mathbf{H}$) $< K$ and assumption (**A3**) does not hold. Hence the proposed method is applicable to the more transmitters case, provided the additional condition $J(L+1) \geq K$ is satisfied. We note that if the channel has more transmitters than receivers, channel equalization and source separation may be difficult even if accurate channel estimate is available. In addition, we note that in the proposed method, the channel impulse response matrix $\mathbf{H}$ is only assumed to be full column rank (**A3**). Hence the channel needs not be irreducible or column reduced.

2.3 Optimal Design of the Precoding Sequence

In Section 2.2, we see that in order to identify the channel, the precoding sequence must be selected so that the resulting matrix $\mathbf{M}_j$ is full column rank such that $\mathbf{F}_j$ can be exactly solved as (2.18). However, when noise is present, the covariance matrix $\mathbf{R}_{\bar{\mathbf{x}}}$ contains the contribution of noise and numerical error is present in the estimation of $\mathbf{R}_{\bar{\mathbf{x}}}$ in practice. This implies that (2.16) usually has no solution and (2.18) becomes a least squares approximate solution. The choice of $\mathbf{M}_j$ will affect error in the computation of $\mathbf{F}_j$ since different $\mathbf{M}_j^T\mathbf{M}_j$ in (2.18) usually have different condition numbers. In this section, we discuss the optimal design of the precoding sequence, which takes into account the effect of noise and numerical error in estimating $\hat{\mathbf{R}}_{\bar{\mathbf{x}}}$, so as to increase the accuracy of $\mathbf{F}_j$ and thus reduce the channel estimation error.

2.3.1 Optimality Criterion

Now we consider the general case that noise is present and discuss the design of the precoding sequence $p(n)$. From (2.4) and assumption (**A1**), the covariance matrix of the received signal is

$$\mathbf{R}_{\bar{\mathbf{x}}} = \mathbf{H}_0\mathbf{G}^2\mathbf{H}_0^* + \mathbf{H}_1\mathbf{G}^2\mathbf{H}_1^* + \sigma_w^2\mathbf{I}_J \otimes \mathbf{I}_P. \tag{2.22}$$

From (2.22) and (2.6), we see that noise has only contribution to the diagonal entries of $\mathbf{R}_{\bar{\mathbf{x}}}(0)$. Therefore the $(L+1)$ decoupled groups of equations in (2.16) remain unchanged,

except for the $j = 0$ group, which becomes

$$\Upsilon_0\left(\mathbf{R}_{\bar{\mathbf{x}}}\right) = \Upsilon_0\left(\mathbf{H}_0\mathbf{G}^2\mathbf{H}_0^* + \mathbf{H}_1\mathbf{G}^2\mathbf{H}_1^*\right) + \sigma_w^2\Upsilon_0\left(\mathbf{I}_J \otimes \mathbf{I}_P\right) = \mathbf{M}_0\mathbf{F}_0 + \mathbf{Y}, \tag{2.23}$$

where $\mathbf{Y} = \sigma_w^2[\mathbf{I}_J \ \mathbf{I}_J \ \cdots \ \mathbf{I}_J]^T \in \mathbb{R}^{JP\times J}$. Thus from (2.18), $\hat{\mathbf{F}}_0$, the least squares approximation of $\mathbf{F}_0$, can be written by

$$\hat{\mathbf{F}}_0 = (\mathbf{M}_0^T\mathbf{M}_0)^{-1}\mathbf{M}_0^T\underbrace{(\mathbf{M}_0\mathbf{F}_0 + \mathbf{Y})}_{\Upsilon_0(\mathbf{R}_{\bar{\mathbf{x}}}(0))} = \mathbf{F}_0 + (\mathbf{M}_0^T\mathbf{M}_0)^{-1}\mathbf{M}_0^T\mathbf{Y} = \mathbf{F}_0 + \mathbf{Z}, \tag{2.24}$$

which is $\mathbf{F}_0$ plus a perturbation term due to noise. The perturbation term $\mathbf{Z}$ is the least squares solution of the equation $\mathbf{M}_0\mathbf{Z} = \mathbf{Y}$. We note that if every column of $\mathbf{Y}$ is orthogonal to every column of $\mathbf{M}_0$, then $\mathbf{Z} = \mathbf{0}$, which implies $\hat{\mathbf{F}}_0 = \mathbf{F}_0$. But that is impossible since the entries of $\mathbf{M}_0$ are positive and those of $\mathbf{Y}$ are nonnegative. Therefore, we seek to appropriately choose the precoding sequence $p(n)$ such that every column of $\mathbf{Y}$ is as close to being orthogonal to that of $\mathbf{M}_0$ as possible. To this end, we first define $\mathbf{q}_{ki}$ and $\mathbf{y}_i$ shown below as the columns of $\mathbf{M}_0$ and $\mathbf{Y}$, respectively:

$$\mathbf{M}_0 = \left[\underbrace{\mathbf{q}_{01} \ \mathbf{q}_{02} \ \cdots \ \mathbf{q}_{0J}}_{\mathbf{M}_0(:,1:J)} \ \underbrace{\mathbf{q}_{11} \ \mathbf{q}_{12} \ \cdots \ \mathbf{q}_{1J}}_{\mathbf{M}_0(:,J+1:2J)} \ \cdots \ \underbrace{\mathbf{q}_{L1} \ \mathbf{q}_{L2} \ \cdots \ \mathbf{q}_{LJ}}_{\mathbf{M}_0(:,LJ+1:(L+1)J)}\right], \tag{2.25}$$

$$\mathbf{Y} = \sigma_w^2[\mathbf{I}_J \ \mathbf{I}_J \ \cdots \ \mathbf{I}_J]^T = [\mathbf{y}_1 \ \mathbf{y}_2 \ \cdots \ \mathbf{y}_J]. \tag{2.26}$$

Then, due to the special structure of the block matrix $\mathbf{M}_0$ and $\mathbf{Y}$, it is easy to check that $\mathbf{q}_{ki}$ is orthogonal to $\mathbf{y}_j$, i.e., $\mathbf{q}_{ki}^T\mathbf{y}_j = 0$ for $j \neq i$, e.g.,

$$\mathbf{q}_{01}^T\mathbf{y}_2 = [\underbrace{p(0)^2\ 0\ \cdots\ 0}_{J\ entries} \cdots \underbrace{p(P-1)^2\ 0\ \cdots\ 0}_{J\ entries}][\underbrace{0\ \sigma_w^2\ 0\ \cdots 0}_{J\ entries} \cdots \underbrace{0\ \sigma_w^2\ 0\ \cdots 0}_{J\ entries}]^T = 0,$$

and each $\mathbf{q}_{ki}^T\mathbf{y}_i$ assumes the same value, $\sigma_w^2\sum_{n=0}^{P-1}p(n)^2$, for $k = 0, 1, \cdots, L$, $i = 1, 2, \cdots, J$, e.g.,

$$\mathbf{q}_{01}^T\mathbf{y}_1 = [\underbrace{p(0)^2\ 0\ \cdots\ 0}_{J\ entries} \cdots \underbrace{p(P-1)^2\ 0\ \cdots\ 0}_{J\ entries}][\underbrace{\sigma_w^2\ 0\ \cdots 0}_{J\ entries} \cdots \underbrace{\sigma_w^2\ 0\ \cdots 0}_{J\ entries}]^T = \sigma_w^2\sum_{n=0}^{P-1}p(n)^2.$$

Thus we only need to consider the relation between columns of $\mathbf{q}_{01}$ and $\mathbf{y}_1$ (the case of $k = 0$ and $i = 1$). Define the correlation coefficient

$$\gamma = \frac{\mathbf{q}_{01}^T\mathbf{y}_1}{\|\mathbf{q}_{01}\|_2\|\mathbf{y}_1\|_2}. \tag{2.27}$$

Since γ is nonnegative and by Cauchy-Schwarz inequality, $0 \leq \gamma \leq 1$. In order to make the perturbation term $\mathbf{Z}$ small, we choose $\mathbf{q}_{01}$ so that the correlation coefficient γ is as small

as possible. Based on this point of view, we formulate the optimal selection problem as minimizing γ subject to

$$\frac{1}{P}\sum_{n=0}^{P-1}|p(n)|^2 = 1, \tag{2.28}$$

$$|p(n)|^2 \geq \tau > 0, \qquad \forall\, 0 \leq n \leq P-1. \tag{2.29}$$

Roughly, constraint (2.28) normalizes the power gain of the precoding sequence of each transmitter to 1; constraint (2.29) requires that at each instant, the power gain is no less than τ. Note that the problem of selecting the precoding sequence is identical to the SISO case considered in [16]. Thus the optimal precoding sequence $p(n)$ is a two-level sequence with a single peak in one period [16]. More specifically, for each m, $0 \leq m \leq P-1$,

$$p(n) = \begin{cases} \sqrt{P(1-\tau)+\tau}\,, & n = m \\ \sqrt{\tau}\,, & n \neq m,\ \ 0 \leq n \leq P-1 \end{cases} \tag{2.30}$$

is an optimal precoding sequence. Because the precoding sequence is periodic with period P, the single peak can be placed at any one of the P positions which yield the same $\gamma = \frac{1}{\sqrt{P(1-\tau)^2+\tau(2-\tau)}}$. Note that γ decreases as τ decreases, which implies that the noise effect in the estimation of covariance matrix $\mathbf{R}_{\bar{\mathbf{x}}}$ is minimized and thus identification performance improves. However the peak location m does significantly affect the numerical condition of the linear equation (2.16). We discuss the selection of m next.

2.3.2 On Selection of m

We now consider the selection of m. We know that different choices of m result in different matrix $\mathbf{M}_j$ and affect the numerical computation of $\mathbf{F}_j, j = 1, 2, \cdots, L$, in (2.18) and $\hat{\mathbf{F}}_0$ in (2.24), since different $\mathbf{M}_j^T\mathbf{M}_j$ may have different condition number. If the condition number is large, then the matrix $\mathbf{M}_j^T\mathbf{M}_j$ is ill-conditioned and the computations in (2.18) and (2.24) are sensitive to data error. Let

$$\mu = \max_{0\leq j\leq L} \kappa(\mathbf{M}_j^T\mathbf{M}_j), \tag{2.31}$$

where $\kappa(\mathbf{A})$ is the condition number of $\mathbf{A}$. Our goal is to choose m so as to minimize the largest condition number of the corresponding matrices $\mathbf{M}_j^T\mathbf{M}_j$, $j = 0, 1, \cdots, L$. Since the peak appears at one of the P possible positions in the periodic precoding sequence, there are P precoding sequences which may result in P different μ. The following result shows that some choices of m are to be avoided since they result in some $\mathbf{M}_j$ being rank deficient and thus $\mu = \infty$.

Proposition 2.2 : At least one $\mathbf{M}_j$, $0 \leq j \leq L$, is not full column rank if and only if $P - L + 1 \leq m \leq P - 2$.
Proof : See Appendix A.

Hence if we choose, either $0 \leq m \leq P - L$ or $m = P - 1$, then each $\mathbf{M}_j$ is full column rank and the channel is identifiable. The following result shows that we can classify the remaining choices into 2 groups that are relevant to the optimal choice of m.
Proposition 2.3 :
(a) Each of the $(P - L)$ choices, $m = 0$, $m = 1, \cdots, m = P - L - 1$, results in the same μ denoted by μ_1.
(b) The two choices $m = P - L$ and $m = P - 1$ result in the same μ denoted by μ_2. Also $\mu_2 \geq \mu_1$.
Proof : See Appendix A.

From Proposition 2.3, we know if $\mu_2 > \mu_1$, then we choose case (a); if $\mu_2 = \mu_1$, we proceed to compare the second largest condition numbers of the set of matrices $\{\mathbf{M}_j^T \mathbf{M}_j\}_{j=0}^{L}$ for these two cases and choose the case whose value is smaller. If they are again equal, the same procedure can be done by comparing the third largest condition numbers and so on. Moreover, for $0 \leq m \leq P - L - 1$ (case (a)), since the condition numbers of $\mathbf{M}_j^T \mathbf{M}_j$ are the same for each fixed j, $j = 0, 1, \cdots, L$, (see Appendix A), we can use $m = 0$ to represent case (a). Similarly, $m = P - 1$ can be used to represent case (b). Hence the optimal selection of m reduces to one of two cases: $m = 0$ or $m = P - 1$. In other words, the optimal precoding sequence has a peak either at the beginning or at the end.

2.4 Identification Algorithm

So far, we have proposed a method for blind identification of FIR MIMO channels using periodic precoding sequence. It is shown that, by properly choosing the precoding sequence, the MIMO FIR transfer functions, with K inputs and J outputs, can be identified up to a unitary matrix ambiguity. The proposed algorithm requires solving linear equations and computing the nonzero eigenvalues and eigenvectors of a Hermitian positive semidefinite matrix. Since the cyclostationarity is induced at the transmitter, the identifiability condition imposed on the channel is minimum: it only requires that channel impulse response matrix $\mathbf{H}$ is full column rank. The channel transfer matrix is not required to be irreducible or column reduced. The channel can have more receivers or more transmitters. The performance of the algorithm depends on the precoding sequence which is optimally designed to reduce the effect of noise and error in estimating the covariance matrix of the received data.

We summarize the proposed method as the following algorithm.
1) Use the precoding sequence $p(n)$ in (2.30) with optimal selection of $m = 0$ or $m = P-1$ to form the matrix $\mathbf{M}_j$ in (2.17).
2) Estimate the covariance matrix $\mathbf{R}_{\bar{\mathbf{x}}}$ via the time average $\hat{\mathbf{R}}_{\bar{\mathbf{x}}} = \frac{1}{S}\sum_{i=1}^{S} \bar{\mathbf{x}}(i)\bar{\mathbf{x}}(i)^*$, where S is the number of data block (i.e., SP is the number of samples for each transmitter).
3) Compute $\mathbf{F}_j$, formed by the channel product matrices, for $j = 0, 1, \cdots, L$, using (2.18).
4) Form the matrix $\mathbf{Q}$ as in (2.19), and obtain the channel impulse response matrix (2.21) by computing the K largest eigenvalues and the associated eigenvectors of $\mathbf{Q}$.

2.5 Simulation Results

In this section, we use several examples to demonstrate the performance of the proposed method. The channel normalized root-mean-square error (NRMSE) is defined as

$$\text{NRMSE} = \frac{1}{\|\mathbf{H}\|_F}\sqrt{\frac{1}{I}\sum_{i=1}^{I}\|\widehat{\mathbf{H}}^{(i)} - \mathbf{H}\|_F^2}, \tag{2.32}$$

where $\|\cdot\|_F$ denotes the Frobenius norm. $\widehat{\mathbf{H}}^{(i)} = [\widehat{\mathbf{H}}^{(i)}(0)^T\ \widehat{\mathbf{H}}^{(i)}(1)^T\ \cdots\ \widehat{\mathbf{H}}^{(i)}(L)^T]^T$ is the estimate of channel impulse response matrix $\mathbf{H}$ after removing the unitary matrix ambiguity by the least squares method [21]. $I = 100$ is the number of Monte Carlo runs. The input source symbols are independent and identically distributed (i.i.d.) QPSK signals. The channel noise is temporally and spatially white Gaussian. The signal-to-noise ratio (SNR) at the output is defined as $\text{SNR} = \frac{\frac{1}{P}\sum_{n=0}^{P-1} E[\|\mathbf{t}(n)\|_2^2]}{E[\|\mathbf{w}(n)\|_2^2]}$, where $\mathbf{t}(n) = [t_1(n)\ \cdots\ t_J(n)]^T$ is the signal component of the received signal (see Figure 2.1).

1) Simulation 1 – optimal selection of precoding sequences

In this simulation, we use the following model

$$\begin{aligned}\mathbf{H}(z) = &\underbrace{\begin{bmatrix} 1.34 - 0.55i & 1.67 + 0.12i \\ -0.69 + 0.25i & -0.51 - 0.33i \end{bmatrix}}_{\mathbf{H}(0)} + \underbrace{\begin{bmatrix} -1.45 + 0.21i & -1.35 + 0.21i \\ 0.62 - 0.31i & -0.76 + 0.43i \end{bmatrix}}_{\mathbf{H}(1)} z^{-1} \\ &+ \underbrace{\begin{bmatrix} -0.31 + 0.15i & -0.41 - 0.16i \\ -0.29 + 0.21i & -0.25 - 0.14i \end{bmatrix}}_{\mathbf{H}(2)} z^{-2}\end{aligned} \tag{2.33}$$

to demonstrate the effect of different precoding sequences on the performance of the proposed method. In experiment 1, the first sequence is chosen as $\{0.767\ 1.07\ 1.07\ 1.07\}$, which satisfies (2.28) and (2.29). The second and third sequences are chosen based on

(2.30) for $P = 4$ and $\tau = 0.5878$ with the two possible peak positions: $m = 0$ and $m = 3$. By computation, the corresponding μ for the three cases are 40.0, 4.66 and 22.1, respectively. Thus $m = 0$ is the optimal selection. Figure 2.2 shows that for SNR=10 dB, there are about 5∼7 dB and 5∼9 dB difference in NRMSE between the optimal one and two others.

In experiment 2, we use the precoding sequences that satisfy (2.30) with $m = 0$, but with different τ to test the effect of τ on the identification performance. Figure 2.3 shows that for each sequence, when the number of samples (for each transmitter) is fixed at 1000, the NRMSE decreases as SNR increases and is roughly constant for SNR $\geq$ 20 dB. A possible explanation is that for sufficiently large SNR, the NRMSE is contributed mainly by numerical error rather than by channel noise. Figure 2.3 also shows that the identification performs better for smaller τ, which is consistent with the conclusion at the end of Section 2.3.1.

2) Simulation 2 – channel order overestimation

In this simulation, we use the following channel model

$$\mathbf{H}(z) = \underbrace{\begin{bmatrix} 0.4851 & 0.3200 \\ -0.3676 & 0.2182 \end{bmatrix}}_{\mathbf{H}(0)} + \underbrace{\begin{bmatrix} -0.4851 & 0.9387 \\ 0.8823 & 0.8729 \end{bmatrix}}_{\mathbf{H}(1)} z^{-1} + \underbrace{\begin{bmatrix} 0.7276 & -0.1280 \\ 0.2941 & -0.4364 \end{bmatrix}}_{\mathbf{H}(2)} z^{-2} \tag{2.34}$$

given in [19]. For each upper bound $\hat{L}$, $0 \leq (\hat{L} - L) \leq 6$, we choose $P = \hat{L} + 2$, SNR=10 dB, and 1000 samples (for each transmitter) for simulation. The precoding sequences are chosen as (2.30) with $m = 0$ and $\tau = 0.2$, 0.4, 0.6, and 0.8. Figure 2.4 shows the NRMSE increases with increasing channel order overestimation. We see the proposed method is quite robust to channel order overestimation when τ is small. For example, with $\tau = 0.4$, when $(\hat{L} - L)$ increases from 0 to 3, the NRMSE increases from -25.5dB to -21dB, which is still a low value.

3) Simulation 3 – a 3-input 2-output channel

In this simulation, we use the 3-input 2-output model

$$\mathbf{H}(z) = \underbrace{\begin{bmatrix} 1.6 & 0.88 & 0.66 \\ 0.8 & 0.44 & 0.33 \end{bmatrix}}_{\mathbf{H}(0)} + \underbrace{\begin{bmatrix} -0.44 & 0.35 & 0.14 \\ -0.14 & 0.37 & 0.23 \end{bmatrix}}_{\mathbf{H}(1)} z^{-1} + \underbrace{\begin{bmatrix} 0.13 & 0.01 & 0.08 \\ 0.26 & 0.02 & 0.16 \end{bmatrix}}_{\mathbf{H}(2)} z^{-2} \tag{2.35}$$

to illustrate the performance of the proposed method for channel with more transmitters than receivers. Note that $\mathbf{H}$ is full column rank, but the channel is not irreducible [21]

because $\mathbf{H}(0)$ is not full rank, and it is not column reduced [21] either because $\mathbf{H}(2)$ is not full rank. In experiment 1, the precoding sequences ($P = 4$) are given as in (2.30) with $m = 0$ and $m = 3$, respectively. Figure 2.5 shows that the NRMSE decreases as the number of data samples increases for SNR=10 dB. As expected, $m = 0$ case (the optimal selection) is better than $m = 3$ case.

In experiment 2, we use the precoding sequences that satisfy (2.30) with $m = 0$, but with different τ to test the effect of τ on the identification performance. Figure 2.6 shows that for each sequence, when the number of samples (for each transmitter) is fixed at 1000, the NRMSE decreases as SNR increases and is roughly constant for SNR $\geq$ 25 dB due to numerical error. Figure 2.6 also shows the identification performs better for smaller τ.

4) Simulation 4 – channel equalization performance

In this simulation, we use the channel model given in (2.34) to demonstrate the performance of the proposed method for channel equalization. We use the precoding sequences that satisfy (2.30) with $m = 0$, but with different τ to test the effect of τ on the equalization performance. For simplicity, we use the minimum mean square error (MMSE) equalizer. The equalizer is a 17-tap Wiener filter with 12-tap reconstruction delay whose jth output $\hat{u}_j(k)$ is an estimate of $u_j(k)$ for $j = 1, 2, \cdots, K$. Since the precoding scheme is applied at the transmitter, we need to multiply $\hat{u}_j(k)$ by the corresponding $p(k)^{-1}$ to obtain an estimate of $s_j(k)$ for $j = 1, 2, \cdots, K$. The number of samples is 1200. We first identify the channel using the first 400 samples and then do equalization. To obtain smoother curves, we use $I = 300$ as the number of Monte Carlo runs rather than 100.

Figure 2.7 shows that under low SNR, the proposed method performs better when τ is large; however, under high SNR, the proposed method performs better when τ is low. A possible explanation is as follows.

Channel estimates become more accurate as τ becomes smaller, but the gains $p(k)^{-1} = \frac{1}{\sqrt{\tau}}$, $k = 1, 2, \cdots, P-1$ become larger and result in larger noise amplification at the receiver. Both channel estimation error and channel noise contribute to the (maximum likelihood) detection performance, i.e., the symbol error rate. In the low SNR region, the detrimental effect of noise amplification outweighs the benefit of small estimation error; whereas in the high SNR region, accurate channel estimation weighs more than the noise amplification effect. Hence we choose a small τ when SNR is high and a large τ when SNR is low.

5) Simulation 5 – Comparisons with other methods

In this simulation, we generate 100 2-input 4-output random channels with order $L = 2$; each element in the channel impulse response matrix is a complex circular Gaussian random

variable with unit variance. We compare the proposed method with a generalized space time block codes (GSTBC)[23] based method. Both methods require periodic precoding sequences. For the proposed method, the precoding sequence is chosen as {1.500 0.767 0.767 0.767}; whereas the entries in the precoding sequence for the GSTBC method is chosen as random entries with modulus 1 for each random channel simulation [23]. The performance of the proposed method is also compared with a linear prediction (LP)[2, chap. 6] based method, and an outer product decomposition algorithm (OPDA)[20]. Both methods do not require a periodic precoder. MMSE equalizers are used for the proposed method, LP method, and OPDA method. For the GSTBC method, we use the customized equalizer proposed in [23]. Figure 2.8(a) shows that when the number of samples is 1200 (for each transmitter), the identification performance of the proposed method is better than those of the other three methods excepting the GSTBC method for SNR $\geq$ 13 dB. However, Figure 2.8(b) shows the equalization performance of the proposed method is only better than those of the LP and OPDA methods and worse than the GSTBC method. The inconsistency of the channel estimation and equalization performance of the proposed method and the GSTBC method for SNR $\leq$ 13 dB may be due to the different precoding sequences and equalizers used. Figure 2.9 shows that when the number of samples is 200 (for each transmitter), the identification and equalization performance of the proposed method is better than that of the GSTBC method for SNR $\leq$ 15 dB. Figure 2.9 shows that when the number of samples is small, the proposed method has better performance than the GSTBC method under low SNR.

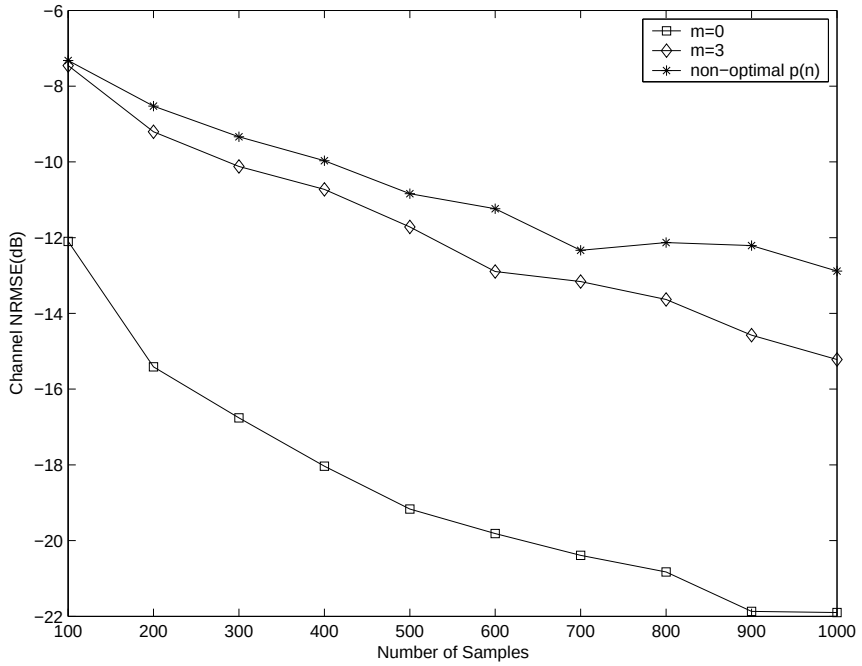

Figure 2.2. Channel NRMSE versus number of samples

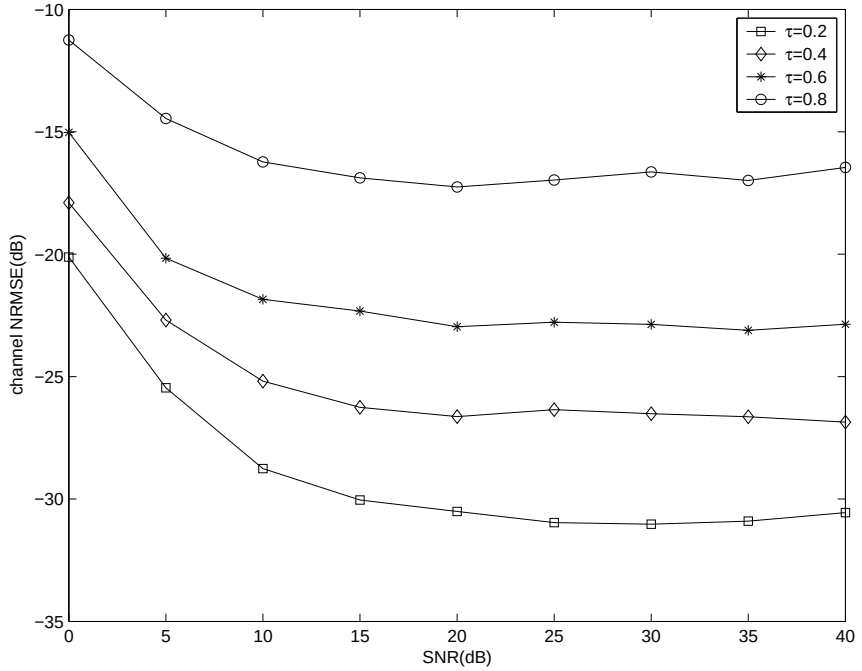

Figure 2.3. Channel NRMSE versus output SNR

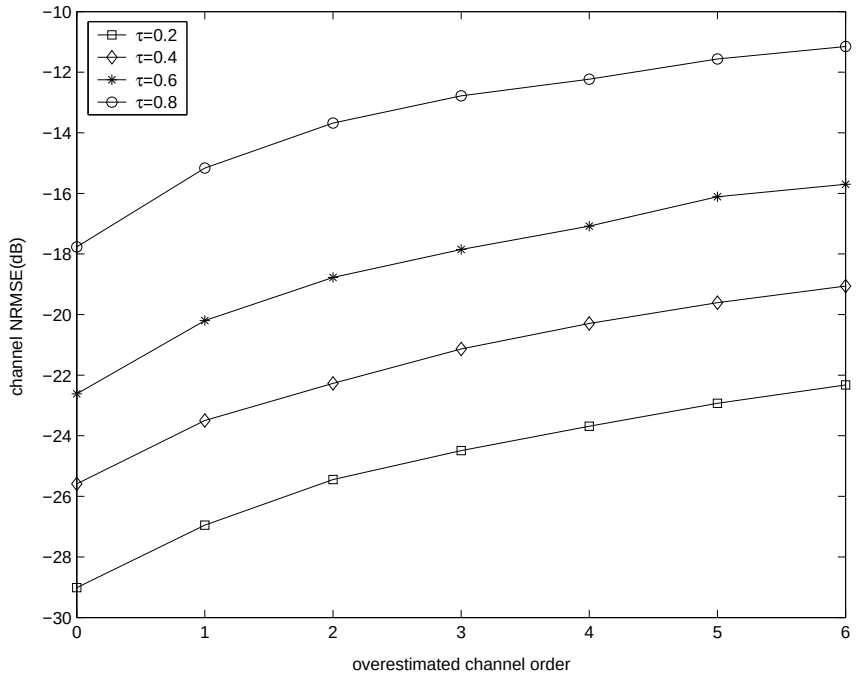

Figure 2.4. Channel NRMSE versus $(\hat{L} - L)$

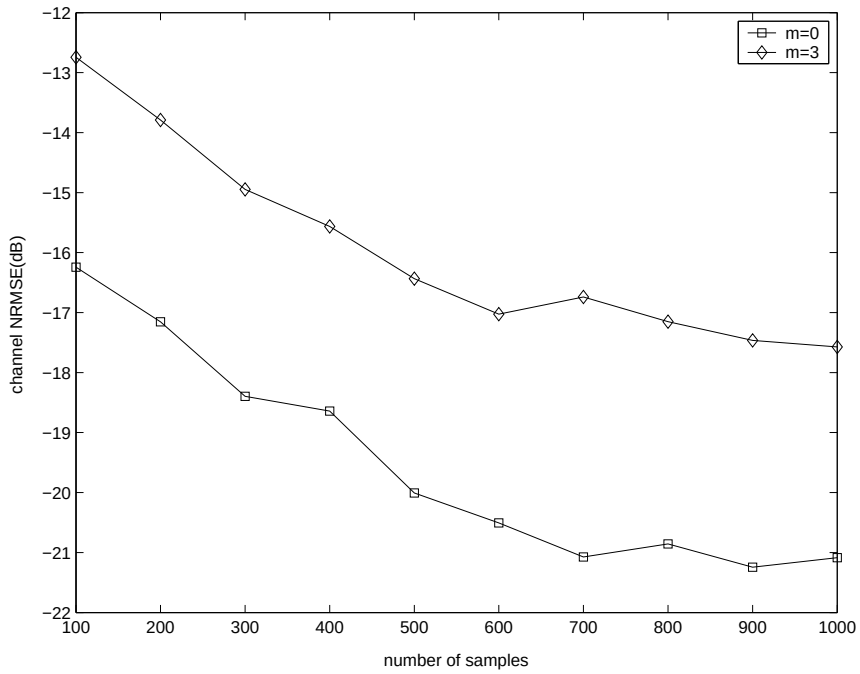

Figure 2.5. 3-input 2-output model: channel NRMSE versus number of samples

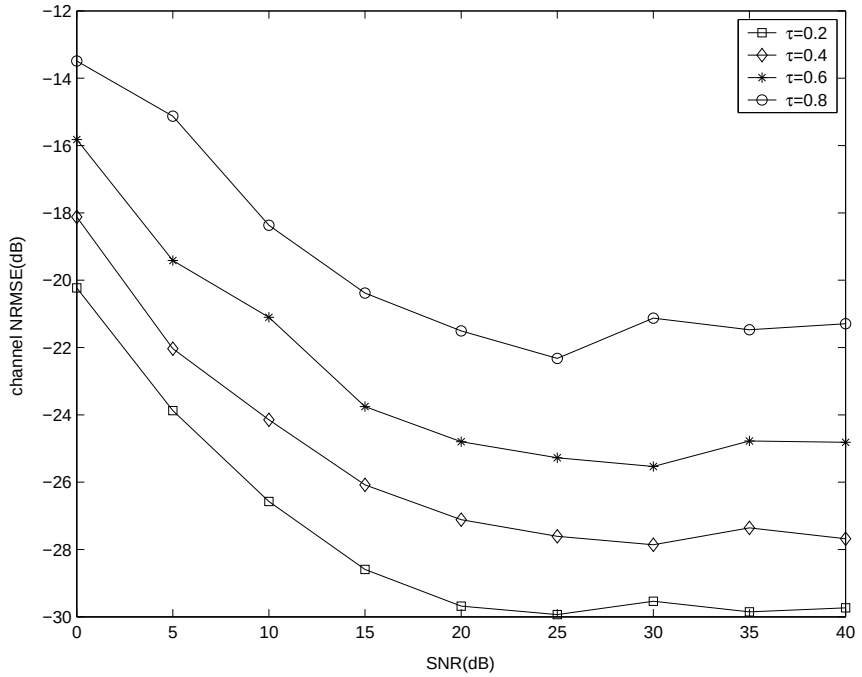

Figure 2.6. 3-input 2-output model: channel NRMSE versus output SNR

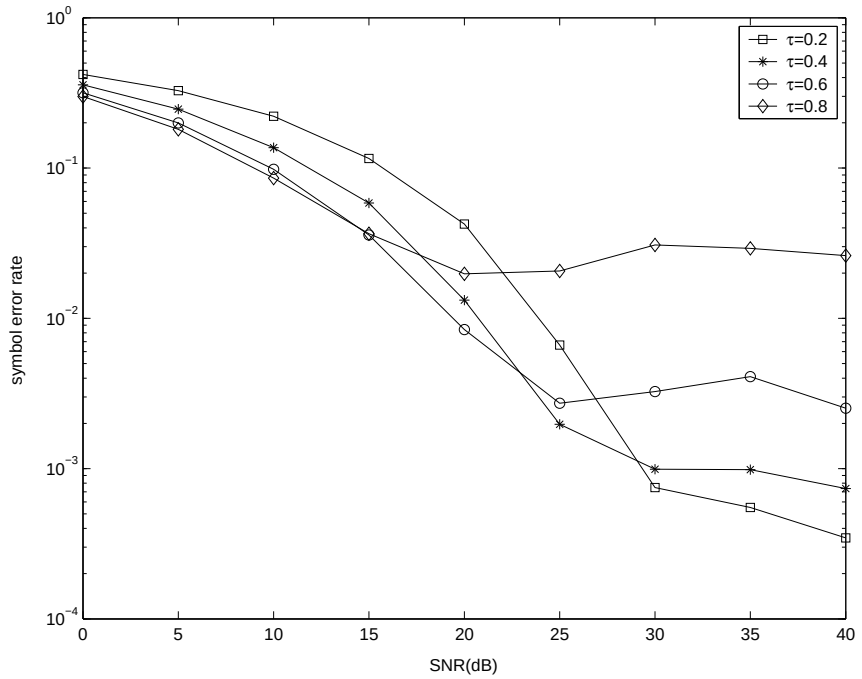

Figure 2.7. Symbol error rate versus output SNR

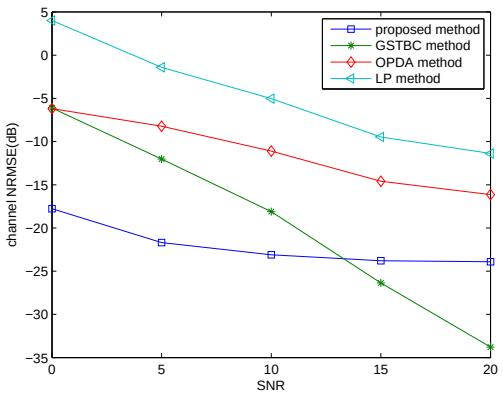

(a) Channel NRMSE versus output SNR

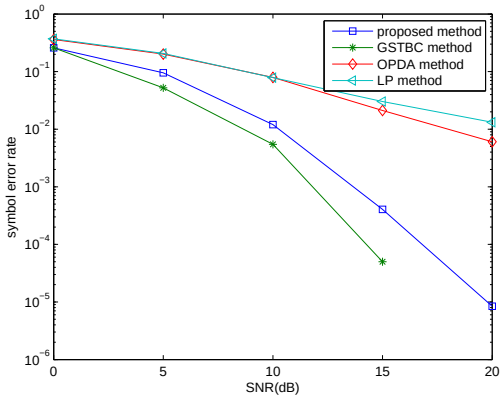

(b) Symbol error rate versus output SNR

Figure 2.8. Comparison of NRMSE and symbol error rate, number of input samples = 1200

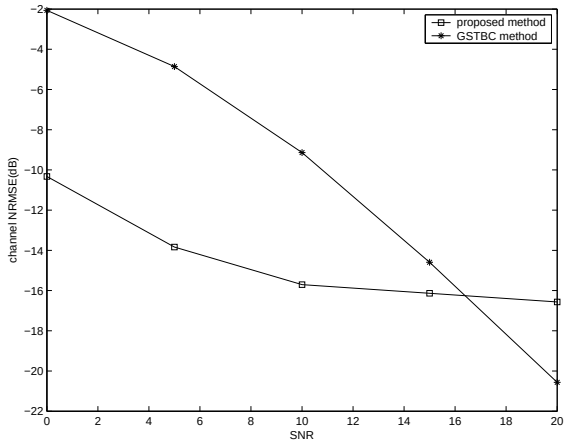

(a) Channel NRMSE versus output SNR

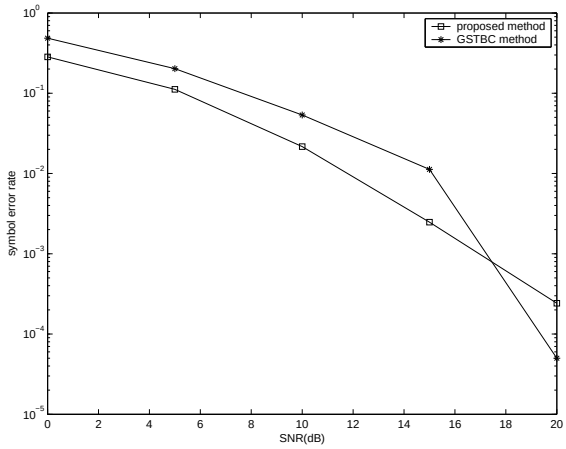

(b) Symbol error rate versus output SNR

Figure 2.9. Comparison of NRMSE and symbol error rate, number of input samples = 200

Chapter 3

Identification of MIMO Single Carrier Zero Padding Channels

In this chapter, we propose a blind identification method based on periodic precoding for another transmission systems, single carrier with zero padding block transmission systems. The method uses periodic precoding on the source signal before transmission. The estimation of the channel impulse response matrix consists of two steps: (1) obtain the channel product matrix by solving a lower-triangular linear system and (2) obtain the channel impulse response matrix by computing the positive eigenvalues and eigenvectors of a Hermitian matrix formed from the channel product matrix. The method is applicable to MIMO channels with more transmitters or more receivers. A sufficient condition for identifiability is simply that the channel impulse response matrix is full column rank. The design of the precoding sequence which minimizes the noise effect in covariance matrix estimation is proposed and the effect of the optimal precoding sequence on channel equalization is discussed. Simulations are used to demonstrate the performance of the method.

3.1 System Model and Formulation

Consider the K-input J-output discrete time SC-ZP block transmission baseband model shown in Figure 3.1. At the transmitter, the kth input signal $v_k(n)$ is first multiplied by a positive P-periodic sequence, $p(n) \in \mathbb{R}$, to obtain $s_k(n) = p(n)v_k(n)$, where $p(n+P) = p(n)$, $\forall\, n$. Then $s_k(n)$ is passed through a serial-to-parallel block whose output is

$$\bar{\mathbf{s}}_k(i) = [s_k(iM) \;\; s_k(iM+1) \;\; \cdots \;\; s_k(iM+M-1)]^T. \tag{3.1}$$

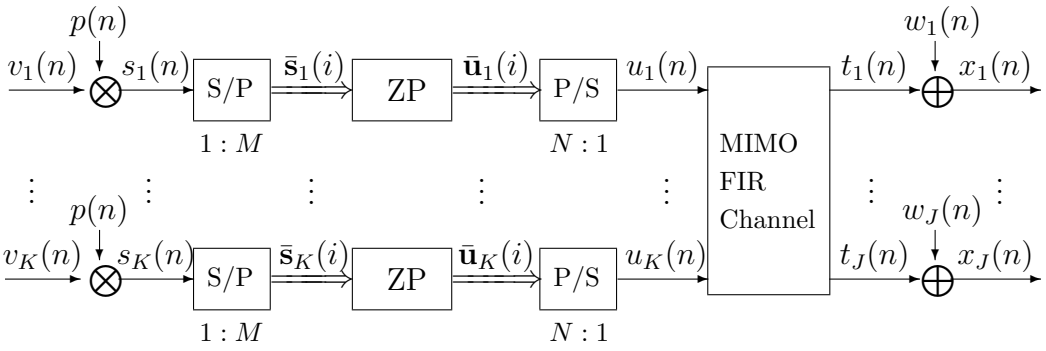

Figure 3.1. An MIMO SC-ZP block transmission baseband model with periodic precoding

Then $\bar{\mathbf{s}}_k(i)$ is passed through a zero padding prefilter $\mathbf{F}_1 = [\mathbf{I}_M \ \mathbf{0}_{P\times M}^T]^T \in \mathbb{R}^{(M+P)\times M}$ whose output is

$$\bar{\mathbf{u}}_k(i) = \mathbf{F}_1\bar{\mathbf{s}}_k(i) = [\ \underbrace{\bar{\mathbf{s}}_k(i)^T}_{M \ \ entries} \ \underbrace{0\cdots 0}_{P \ \ entries}\ ]^T = [\underbrace{u_k(iN)\cdots u_k(iN+M-1)}_{M \ \ entries} \ \underbrace{0\cdots 0}_{P \ \ entries}\ ]^T, \quad (3.2)$$

where $N = M + P$. Finally, $\bar{\mathbf{u}}_k(i)$ is converted to $u_k(n)$ via a parallel-to-serial block and transmitted through the MIMO FIR channel. At the receiver, the jth received signal is $x_j(n) = t_j(n) + w_j(n)$, where $t_j(n)$ is the signal component at the output and $w_j(n)$ is the channel noise seen at the jth receiver. If we define $\mathbf{x}(n) = [x_1(n) \ x_2(n) \ \cdots \ x_J(n)]^T \in \mathbb{C}^J$, then $\mathbf{x}(n)$ can be written as

$$\mathbf{x}(n) = \sum_{l=0}^{L} \mathbf{H}(l)\mathbf{u}(n-l) + \mathbf{w}(n) = \mathbf{t}(n) + \mathbf{w}(n), \quad (3.3)$$

where $\mathbf{u}(n) \in \mathbb{C}^K$, $\mathbf{w}(n) \in \mathbb{C}^J$, and $\mathbf{t}(n) \in \mathbb{C}^J$ are similarly defined as $\mathbf{x}(n)$, and $\mathbf{H}(l) \in \mathbb{C}^{J\times K}$ is the channel coefficient matrix whose jkth element $h_{jk}(l)$, $l = 0, 1, \cdots, L_{jk}$, is the impulse response from the kth transmitter to the jth receiver, and $L = \max_{j,k}\{L_{jk}\}$ is the order of the MIMO channel. We assume that $\mathbf{H}(L) \neq \mathbf{0}_{J\times K}$. Group the sequence of $\mathbf{x}(n)$ as $\bar{\mathbf{x}}(i) = [\mathbf{x}(iN)^T \ \mathbf{x}(iN+1)^T \cdots \mathbf{x}(iN+N-1)^T]^T \in \mathbb{C}^{JN}$, and define $\bar{\mathbf{u}}(i) \in \mathbb{C}^{KN}$ and $\bar{\mathbf{w}}(i) \in \mathbb{C}^{JN}$ similarly as $\bar{\mathbf{x}}(i)$, we have

$$\bar{\mathbf{x}}(i) = \mathbf{H_0}\bar{\mathbf{u}}(i) + \mathbf{H_1}\bar{\mathbf{u}}(i-1) + \bar{\mathbf{w}}(i), \quad (3.4)$$

where $\mathbf{H_0}$ is a $JN \times KN$ block lower-triangular Toeplitz matrix with the first block column being $[\mathbf{H}(0)^T \ \mathbf{H}(1)^T \cdots \mathbf{H}(L)^T \ \mathbf{0}_{J\times K}^T \cdots \mathbf{0}_{J\times K}^T]^T \in \mathbb{C}^{JN\times K}$, and $\mathbf{H_1}$ is a $JN \times KN$ block upper-triangular Toeplitz matrix with the first block row being $[\mathbf{0}_{J\times K} \cdots \mathbf{0}_{J\times K} \ \mathbf{H}(L) \ \mathbf{H}(L-1)\cdots\mathbf{H}(1)] \in \mathbb{C}^{J\times KN}$. We assume that the receivers are synchronized with the transmitters. In addition, the following assumptions are made throughout this chapter.

(**B1**) The source signal $\mathbf{v}(n) = [v_1(n)\ v_2(n)\ \cdots\ v_K(n)]^T \in \mathbb{C}^K$ is a zero mean white sequence with $E[\mathbf{v}(m)\mathbf{v}(n)^*] = \delta(m-n)\mathbf{I}_K \in \mathbb{R}^{K\times K}$, where $\delta(\cdot)$ is the Kronecker delta function. The noise is white zero mean with $E[\mathbf{w}(m)\mathbf{w}(n)^*] = \delta(m-n)\sigma_w^2\mathbf{I}_J \in \mathbb{R}^{J\times J}$. In addition, the source signal is uncorrelated with the noise $\mathbf{w}(n)$, i.e., $E[\mathbf{v}(m)\mathbf{w}(n)^*] = \mathbf{0}_{K\times J}$, $\forall\, m, n$.

(**B2**) An upper bound $\hat{L}$ of the channel order L is known, $P = \hat{L} + 1$, and $M > P$ is a multiple of P.

(**B3**) The channel impulse response matrix $\mathbf{H} = [\mathbf{H}(0)^T\ \mathbf{H}(1)^T \cdots \mathbf{H}(L)^T]^T$ is full column rank, i.e., $\text{rank}(\mathbf{H}) = K$.

In the next section, we derive an algorithm for blind identification of the MIMO channel impulse response matrix $\mathbf{H}$ using second-order statistics of the received data.

3.2 Blind Channel Identification

In this section, we derive the proposed method under assumptions (**B1**), (**B2**), and (**B3**). We discuss an optimal design of the precoding sequence, which takes into account the noise effect in the estimation of covariance matrix of the received data, so as to increase the accuracy in the computation of the channel product matrix $\mathbf{HH}^*$ and thus reduce the channel estimation error. With the proposed optimal precoding sequence, the computation of $\mathbf{HH}^*$ becomes particularly simple. Taking eigen-decomposition of $\mathbf{HH}^*$, we obtain the channel impulse response matrix $\mathbf{H}$ up to a unitary matrix ambiguity.

3.2.1 The Identification Method

We first derive the proposed method for the case where the channel order L is known with $P = L+1$, there are more receivers, i.e., $J \geq K$, and the noise is absent. The cases of channel order overestimation and more transmitters than receivers (i.e., $K > J$) are given at the end of this sub-section. The effects of noise and optimal design of the precoding sequence are discussed in Section 3.2.2.

From (3.4), we know that only the last L block columns of $\mathbf{H_1}$ are non-zero and zeros are padded in the last P block rows of $\bar{\mathbf{u}}(i-1)$ and $\bar{\mathbf{u}}(i)$ (see (3.2)). Hence the product $\mathbf{H_1}\bar{\mathbf{u}}(i-1)$ equals the zero vector and (3.4) can be written as follows (noiseless case):

$$\overbrace{\begin{bmatrix} \mathbf{x}(iN) \\ \vdots \\ \mathbf{x}(iN+L) \\ \vdots \\ \mathbf{x}(iN+M-1) \\ \vdots \\ \mathbf{x}(iN+N-1) \end{bmatrix}}^{\bar{\mathbf{x}}(i)} = \overbrace{\begin{bmatrix} \mathbf{H}(0) & & & & \\ \vdots & \ddots & & & \\ \mathbf{H}(L) & \cdots & \mathbf{H}(0) & & \\ & \ddots & \vdots & \ddots & \\ & & \mathbf{H}(L) & \cdots & \mathbf{H}(0) \\ & & & \ddots & \vdots \\ & & & & \mathbf{H}(L) \cdots \mathbf{H}(0) \end{bmatrix}}^{\mathbf{H_0}} \overbrace{\begin{bmatrix} \mathbf{u}(iN) \\ \vdots \\ \mathbf{u}(iN+L) \\ \vdots \\ \mathbf{u}(iN+M-1) \\ \mathbf{0} \\ \vdots \\ \mathbf{0} \end{bmatrix}}^{\bar{\mathbf{u}}(i)} = \mathbf{H_e}\bar{\mathbf{s}}(i), \tag{3.5}$$

where $\mathbf{H_e}$ is the sub-matrix formed from the first M block columns of $\mathbf{H_0}$ and $\bar{\mathbf{s}}(i) = [\mathbf{u}(iN)^T\, \mathbf{u}(iN+1)^T\, \cdots\, \mathbf{u}(iN+M-1)^T]^T$ is the first M block entries of $\bar{\mathbf{u}}(i)$. Because $\mathbf{u}(iN) = [u_1(iN)\ u_2(iN)\ \cdots\ u_K(iN)]^T$ (see the line below (3.3)) and $u_k(iN) = s_k(iM)$ for $k = 1, 2, \cdots, K$ (see (3.2)), $\mathbf{u}(iN) = [s_1(iM)\, s_2(iM)\, \cdots\ s_K(iM)]^T \triangleq \mathbf{s}(iM)$. Similarly, $\mathbf{u}(iN+m) = \mathbf{s}(iM+m)$ for $m = 1, 2, \cdots, M-1$. Hence $\bar{\mathbf{s}}(i) = [\mathbf{s}(iM)^T\, \mathbf{s}(iM+1)^T\, \cdots\, \mathbf{s}(iM+M-1)^T]^T$.

Let $\mathbf{x}_f(i) = [\mathbf{x}(iN)^T\ \mathbf{x}(iN+1)^T\ \cdots\ \mathbf{x}(iN+L)^T]^T$ be the first $J(L+1)$ rows of $\bar{\mathbf{x}}(i)$. Then

$$\mathbf{x}_f(i) = \mathbf{H}_f \mathbf{s}_f(i), \tag{3.6}$$

where $\mathbf{H}_f \in \mathbb{C}^{J(L+1)\times K(L+1)}$ is the sub-matrix formed from the first $(L+1)$ block columns and block rows of $\mathbf{H_e}$, and $\mathbf{s}_f(i) = [\mathbf{s}(iM)^T\ \mathbf{s}(iM+1)^T\ \cdots\ \mathbf{s}(iM+L)^T]^T$. Also we know for $k = 1, 2, \cdots, K$, $s_k(iM) = p(iM)v_k(iM) = p(0)v_k(iM)$ from (3.1) and assumption (**B2**). Hence $\mathbf{s}(iM) = [p(0)v_1(iM)\ p(0)v_2(iM)\ \cdots\ p(0)v_K(iM)]^T = p(0)\mathbf{v}(iM)$, where $\mathbf{v}(iM) = [v_1(iM)\ v_2(iM)\ \cdots\ v_K(iM)]^T$. Similarly, $\mathbf{s}(iM+n) = p(n)\mathbf{v}(iM+n)$ for $n = 1, 2, \cdots, L$. Therefore (3.6) can be written as

$$\overbrace{\begin{bmatrix} \mathbf{x}(iN) \\ \mathbf{x}(iN+1) \\ \vdots \\ \mathbf{x}(iN+L) \end{bmatrix}}^{\mathbf{x}_f(i)} = \overbrace{\begin{bmatrix} p(0)\mathbf{H}(0) & & \\ p(0)\mathbf{H}(1) & p(1)\mathbf{H}(0) & \\ \vdots & \vdots & \ddots \\ p(0)\mathbf{H}(L) & p(1)\mathbf{H}(L-1) \cdots & p(L)\mathbf{H}(0) \end{bmatrix}}^{\mathbf{H}_p} \overbrace{\begin{bmatrix} \mathbf{v}(iM) \\ \mathbf{v}(iM+1) \\ \vdots \\ \mathbf{v}(iM+L) \end{bmatrix}}^{\mathbf{v}_f(i)}. \tag{3.7}$$

Define $\mathbf{S} \in \mathbb{R}^{J(L+1)\times J(L+1)}$ as the matrix whose first block sub-diagonal entries are all $\mathbf{I}_J$ (i.e., $\mathbf{S}(J+1 : J(L+1), 1 : JL) = \mathbf{I}_{JL}$), and all remaining entries are zero. Rewrite (3.7) as

$$\mathbf{x}_f(i) = [p(0)\mathbf{H}\ p(1)\mathbf{SH}\ \cdots\ p(L)\mathbf{S}^L\mathbf{H}]\mathbf{v}_f(i) = \mathbf{H}_p\mathbf{v}_f(i). \tag{3.8}$$

Taking expectation of $\mathbf{x}_f(i)\mathbf{x}_f(i)^*$, we get the covariance matrix

$$\mathbf{R}_f = E[\mathbf{x}_f(i)\mathbf{x}_f(i)^*] = \mathbf{H}_p\mathbf{H}_p^* \,. \tag{3.9}$$

From (3.8), since $\mathbf{H}_p = [p(0)\mathbf{H}\ \ p(1)\mathbf{SH}\ \ \cdots\ \ p(L)\mathbf{S}^L\mathbf{H}]$, (3.9) can be written as

$$\mathbf{R}_f = p(0)^2\mathbf{H}\mathbf{H}^* + p(1)^2\mathbf{S}\mathbf{H}\mathbf{H}^*\mathbf{S}^T + \cdots + p(L)^2\mathbf{S}^L\mathbf{H}\mathbf{H}^*(\mathbf{S}^T)^L = \sum_{k=0}^{L} p(k)^2\mathbf{S}^k\mathbf{H}\mathbf{H}^*(\mathbf{S}^T)^k. \tag{3.10}$$

From [37, p.414], we know that the general matrix equation $\sum_{j=1}^{p}\mathbf{A}_j\mathbf{X}\mathbf{B}_j = \mathbf{C}$ can be equivalently expressed as a matrix-vector equation form, $\left[\sum_{j=1}^{p}\mathbf{B}_j^T \otimes \mathbf{A}_j\right]\mathrm{vec}(\mathbf{X}) = \mathrm{vec}(\mathbf{C})$, where $\mathrm{vec}(\cdot)$ is the vec-function which stacks up columns of a matrix. Hence the matrix equation (3.10) can be written in the following vector form:

$$\mathrm{vec}(\mathbf{R}_f) = \mathrm{vec}\left(\sum_{k=0}^{L} p(k)^2\mathbf{S}^k\mathbf{H}\mathbf{H}^*(\mathbf{S}^T)^k\right) = \left(\sum_{k=0}^{L} p(k)^2\mathbf{S}^k \otimes \mathbf{S}^k\right)\mathrm{vec}(\mathbf{H}\mathbf{H}^*) = \mathbf{G}\cdot\mathrm{vec}(\mathbf{H}\mathbf{H}^*). \tag{3.11}$$

Here $\mathbf{G}$ is a block Toeplitz lower-triangular matrix shown as follows:

$$\mathbf{G} = \sum_{k=0}^{L} p(k)^2\mathbf{S}^k \otimes \mathbf{S}^k = \begin{bmatrix} p(0)^2\mathbf{I}_{JF} & \mathbf{0} & \cdots & \mathbf{0} \\ p(1)^2\widehat{\mathbf{S}} & p(0)^2\mathbf{I}_{JF} & \cdots & \mathbf{0} \\ \vdots & \vdots & \ddots & \vdots \\ p(L)^2\widehat{\mathbf{S}}^L & p(L-1)^2\widehat{\mathbf{S}}^{L-1} & \cdots & p(0)^2\mathbf{I}_{JF} \end{bmatrix} \in \mathbb{R}^{F^2\times F^2}, \tag{3.12}$$

where $F = J(L+1)$ and $\widehat{\mathbf{S}} \in \mathbb{R}^{JF\times JF}$ is a block diagonal matrix with $\mathbf{S}$ on the diagonal blocks. Since $\mathbf{G}$ is square, the solution to (3.11) is

$$\mathrm{vec}(\mathbf{H}\mathbf{H}^*) = \mathbf{G}^{-1}\mathrm{vec}(\mathbf{R}_f) \tag{3.13}$$

provided $p(0) \neq 0$. We use the solution obtained in (3.13) to form a Hermitian matrix $\mathbf{Q} = \mathbf{H}\mathbf{H}^*$. Then under the assumption (**B3**), we can obtain the channel impulse response matrix, up to a unitary matrix ambiguity, by choosing the K largest eigenvalues and the associated eigenvectors of $\mathbf{Q}$, like the way at the end of Section 2.2.1.

Remark 1: So far we have assumed that the channel order L is known. If only an upper bound $\hat{L} \geq L$ is available, then following the same process given in this sub-section, we obtain $\mathrm{vec}(\widehat{\mathbf{H}_{\mathbf{ov}}\mathbf{H}_{\mathbf{ov}}^*}) = [\sum_{k=0}^{\hat{L}}\mathbf{S}_k \otimes \mathbf{S}_k]^{-1}\mathrm{vec}(\mathbf{R}_f)$ where $\mathbf{H}_{\mathbf{ov}} = [\mathbf{H}^T\ \underbrace{\mathbf{0}\ \cdots\ \mathbf{0}}_{\hat{L}-L\ \ blocks}]^T \in \mathbb{C}^{J(\hat{L}+1)\times K}$. Then we can also obtain $\mathbf{Q} = \mathbf{H}_{\mathbf{ov}}\mathbf{H}_{\mathbf{ov}}^*$. Note that the last $(\hat{L}-L)$ block columns and block rows of $\mathbf{Q}$ are zero. Then similar to the discussion in Section 2.2.2, we can also identify the channel impulse response matrix.

Remark 2: The proposed method can apply to the case of more transmitters than receivers. Please see the discussion in Section 2.2.3.

3.2.2 Optimal Design of the Precoding Sequence

When the noise is present, the covariance matrix $\mathbf{R}_f$ contains the contribution of noise. Thus (3.9) becomes

$$\mathbf{R}_f = E[\mathbf{x}_f(i)\mathbf{x}_f(i)^*] = \mathbf{H}_p\mathbf{H}_p^* + \sigma_w^2\mathbf{I}_F, \tag{3.14}$$

where $F = J(L+1)$. In this case, (3.11) becomes

$$\mathrm{vec}(\mathbf{R}_f) = \mathbf{G}\cdot\mathrm{vec}(\mathbf{H}\mathbf{H}^*) + \sigma_w^2\mathrm{vec}(\mathbf{I}_F). \tag{3.15}$$

From (3.13), the approximate solution of $\mathrm{vec}(\mathbf{H}\mathbf{H}^*)$ is

$$\widehat{\mathrm{vec}(\mathbf{H}\mathbf{H}^*)} = \mathbf{G}^{-1}\mathrm{vec}(\mathbf{R}_f). \tag{3.16}$$

It follows from (3.16) and (3.15) that

$$\widehat{\mathrm{vec}(\mathbf{H}\mathbf{H}^*)} = \mathrm{vec}(\mathbf{H}\mathbf{H}^*) + \sigma_w^2\underbrace{\mathbf{G}^{-1}\cdot\mathrm{vec}(\mathbf{I}_F)}_{\mathbf{z}} = \mathrm{vec}(\mathbf{H}\mathbf{H}^*) + \sigma_w^2\mathbf{z}. \tag{3.17}$$

The vector $\mathbf{z} = [z_1\ z_2\ \cdots\ z_{F^2}]^T$ in (3.17) is the solution of $\mathbf{G}\mathbf{z} = \mathrm{vec}(\mathbf{I}_F)$. Since the matrix $\mathbf{G}$ is completely determined by the precoding sequence $p(n)$, we seek to choose $p(n)$ so that $\|\mathbf{z}\|_2^2$ is minimized. To this end, we need to analyze the relations between $\mathbf{z}$ and $p(n)$. By expanding the matrix equation $\mathbf{G}\mathbf{z} = \mathrm{vec}(\mathbf{I}_F)$, we find that

$$\begin{cases} p(0)^2 z_i = 1 \qquad i = 1+k(F+1), \quad k = 0,1,\cdots,J-1 \\ \sum_{n=0}^{1} p(n)^2 z_{i+(1-n)J(F+1)} = 1 \qquad i = 1+k(F+1), \quad k = 0,1,\cdots,J-1 \\ \sum_{n=0}^{2} p(n)^2 z_{i+(2-n)J(F+1)} = 1 \qquad i = 1+k(F+1), \quad k = 0,1,\cdots,J-1 \\ \qquad\vdots \qquad\qquad\qquad\qquad \vdots \qquad\qquad\qquad\qquad \vdots \\ \sum_{n=0}^{L} p(n)^2 z_{i+(L-n)J(F+1)} = 1 \qquad i = 1+k(F+1), \quad k = 0,1,\cdots,J-1 \end{cases} \tag{3.18}$$

and $z_j = 0$ for all other indices j. We write (3.18) as the following matrix equation.

$$\underbrace{\begin{bmatrix} g_0 & 0 & \cdots & 0 \\ g_1 & g_0 & \cdots & 0 \\ \vdots & \vdots & \ddots & \vdots \\ g_L & g_{L-1} & \cdots & g_0 \end{bmatrix}}_{\mathbf{G_s}} \underbrace{\begin{bmatrix} m_0 \\ m_1 \\ \vdots \\ m_L \end{bmatrix}}_{\mathbf{m}} = \underbrace{\begin{bmatrix} 1 \\ 1 \\ \vdots \\ 1 \end{bmatrix}}_{\mathbf{y}} \tag{3.19}$$

where $\mathbf{G_s}$ is a lower-triangular Toeplitz matrix, $g_n = p(n)^2$ for $n = 0,1,\cdots,L$, and $m_j = z_{i+jJ(F+1)}$ for $j = 0,1,\cdots,L$, $i = 1+k(F+1)$, $k = 0,1,\cdots,J-1$. Hence $\mathbf{G}\mathbf{z} = \mathrm{vec}(\mathbf{I}_F)$, the relations between $\mathbf{z}$ and $p(n)$, is reduced to (3.19), and minimization of $\|\mathbf{z}\|_2^2$ is equivalent to minimization of $\|\mathbf{m}\|_2^2$, which is a nonlinear function of $g_0, g_1, \cdots, g_L$. Then the problem

is to minimize $\|\mathbf{m}\|_2^2$ by choosing $g_0, g_1, \cdots, g_L$, subject to suitable constraints. Specifically, we formulate the problem as

$$\text{Minimize}_{g_0,g_1\cdots,g_L}\|\mathbf{m}\|_2^2 \quad \text{subject to}$$

$$g_n \geq \tau > 0, \quad \forall\, 0 \leq n \leq L \tag{3.20}$$

$$\frac{1}{L+1}\sum_{n=0}^{L} g_n = 1 \qquad . \tag{3.21}$$

Roughly, constraint (3.20) requires that at each instant, the power gain ($g_n = p(n)^2$) is no less than τ with $0 < \tau < 1$; constraint (3.21) normalizes the power gain of the precoding sequence of each transmitter to 1.

It is easy to show that for $L = 1$, the problem has a unique global minimizer given by $g_0 = 2 - \tau$ and $g_1 = \tau$. For general $L \geq 2$ case, the standard Kuhn-Tucker conditions [38] of the nonlinear minimization problem do not seem to yield easily a unique analytical solution. However, the problem can be easily solved numerically (for fixed L and τ), say using the *Matlab Optimization Toolbox*. Extensive numerically solutions, with different L, τ, and initial guess, have indicated that a global minimizer exists and is given by

$$g_0 = L + 1 - L\tau, \;\; g_1 = g_2 = \cdots = g_L = \tau. \tag{3.22}$$

In the following, we show that the solution (3.22) is also the global minimizer of an upper bound of $\|\mathbf{m}\|_2^2$. We know $\|\mathbf{m}\|_2^2 = \|\mathbf{G}_\mathbf{s}^{-1}\mathbf{y}\|_2^2 \leq \|\mathbf{G}_\mathbf{s}^{-1}\|_2^2 \cdot \|\mathbf{y}\|_2^2 = (L+1)\|\mathbf{G}_\mathbf{s}^{-1}\|_2^2$, where $\|\mathbf{G}_\mathbf{s}^{-1}\|_2$ is the 2-induced norm of $\mathbf{G}_\mathbf{s}^{-1}$. Since $\mathbf{G}_\mathbf{s}$ is triangular and Toeplitz, it follows from [32] that for any fixed integer $L \geq 1$,

$$\|\mathbf{G}_\mathbf{s}^{-1}\|_2^2 \leq \frac{1}{(\alpha+2)^2\beta^2}[(\alpha+1)^{2(L+1)} + 2(L+1)(\alpha+2) - 1] \triangleq f(\alpha,\beta), \tag{3.23}$$

where $\alpha = \max_{i=1,2,\cdots,L}|\frac{g_i}{g_0}|$ and $\beta = |g_0|$. Hence we know $\|\mathbf{m}\|_2^2 \leq (L+1)f(\alpha,\beta)$. Since for any $\alpha > 0$ and $\beta > 0$, $\frac{\partial f(\alpha,\beta)}{\partial \alpha} > 0$ (see Appendix C) and $\frac{\partial f(\alpha,\beta)}{\partial \beta} = -\frac{2}{\beta}f(\alpha,\beta) < 0$, we know for any fixed $\beta > 0$, $f(\alpha,\beta)$ is an increasing function of α, and for any fixed $\alpha > 0$, $f(\alpha,\beta)$ is a decreasing function of β. Hence to minimize $f(\alpha,\beta)$, we should choose α as small as possible and choose β as large as possible subject to $\beta \leq L + 1 - L\tau$ and $\alpha \geq \frac{\tau}{L+1-L\tau}$. It follows that (3.22) is a global minimizer of the upper bound $(L+1)f(\alpha,\beta)$.

Since $g_n = p(n)^2$ and $p(n) > 0$, the optimal precoding sequence is

$$p(n) = \begin{cases} \sqrt{L+1-L\tau}\,, & n = 0 \\ \sqrt{\tau}\,, & 1 \leq n \leq L \end{cases} \qquad . \tag{3.24}$$

We consider next the effect of τ on channel identification. From (3.19) and [30, 31], we know $\mathbf{m} = \mathbf{G}_\mathbf{s}^{-1}\mathbf{y}$, where $\mathbf{G}_\mathbf{s}^{-1}$ is a lower-triangular Toeplitz matrix with $[\bar{g}_0\ \bar{g}_1\ \cdots\ \bar{g}_L]^T \in$

$\mathbb{R}^{L+1}$ as its first column, and

$$\begin{cases} \bar{g}_0 = \frac{1}{g_0} \\ \bar{g}_l = -\frac{1}{g_0}\sum_{i=1}^{l} \bar{g}_{l-i} g_i, \ \ i = 1, 2, \cdots, l-1, \ \text{ for } \ l = 1, 2, \cdots, L \end{cases} . \tag{3.25}$$

Then

$$\|\mathbf{m}\|_2^2 \ = \ \bar{g}_0^2 + (\bar{g}_0 + \bar{g}_1)^2 + \cdots + (\bar{g}_0 + \bar{g}_1 + \cdots + \bar{g}_L)^2. \tag{3.26}$$

For the optimal solution in (3.22), the corresponding $\bar{g}_n$ in (3.25) can be expressed as follows:

$$\begin{cases} \bar{g}_0 = \frac{1}{L+1-L\tau} > 0 \\ \bar{g}_i = -\frac{\tau}{(L+1-L\tau)^2}(1 - \frac{\tau}{L+1-L\tau})^{i-1} < 0, \qquad i = 1, 2, \cdots, L \end{cases} . \tag{3.27}$$

The following proposition shows that $\|\mathbf{m}\|_2^2$ is a continuous and strictly increasing function of τ on $(0, 1)$. In other words, for $0 < \tau < 1$, $\|\mathbf{m}\|_2^2$ decreases as τ decreases, and thus as τ decreases, the noise effect in the estimation of the covariance matrix $\mathbf{R}_f$ is reduced and hence identification performance improves.

Proposition 3.1: With $\bar{g}_n$ given in (3.27), $\|\mathbf{m}\|_2^2 = \frac{1-(1-\frac{\tau}{L+1-L\tau})^{2(L+1)}}{2(L+1-L\tau)\tau-\tau^2}$ and $\frac{d}{d\tau}\|\mathbf{m}\|_2^2 > 0$ for $0 < \tau < 1$.

Proof: See Appendix D.

3.2.3 Computation of $\mathbf{G}_0^{-1}$

With the precoding sequence $p(n)$ chosen as (3.24), the matrix $\mathbf{G}$ in (3.12) becomes

$$\mathbf{G}_0 = \begin{bmatrix} a\mathbf{I}_{JF} & \mathbf{0} & \cdots & \mathbf{0} \\ b\widehat{\mathbf{S}} & a\mathbf{I}_{JF} & \cdots & \mathbf{0} \\ \vdots & \vdots & \ddots & \vdots \\ b\widehat{\mathbf{S}}^L & b\widehat{\mathbf{S}}^{L-1} & \cdots & a\mathbf{I}_{JF} \end{bmatrix}, \tag{3.28}$$

where $a = L+1-L\tau$, and $b = \tau$. The inverse of $\mathbf{G}_0$ can be obtained by forward substitutions as

$$\mathbf{G}_0^{-1} = \begin{bmatrix} k_0\mathbf{I}_{JF} & \mathbf{0} & \cdots & \mathbf{0} \\ k_1\widehat{\mathbf{S}} & k_0\mathbf{I}_{JF} & \cdots & \mathbf{0} \\ \vdots & \vdots & \ddots & \vdots \\ k_L\widehat{\mathbf{S}}^L & k_{L-1}\widehat{\mathbf{S}}^{L-1} & \cdots & k_0\mathbf{I}_{JF} \end{bmatrix}, \tag{3.29}$$

where $k_0 = \frac{1}{a}$ and $k_i = -\frac{b}{a^2}(1 - \frac{b}{a})^{i-1}$ for $i = 1, 2, \cdots, L$. The solution $\widehat{\text{vec}(\mathbf{HH}^*)} = \mathbf{G}_0^{-1}\text{vec}(\mathbf{R}_f)$ in (3.16) is thus quite easy to compute once the optimal precoding sequence is given.

3.2.4 Identification Algorithm

So far, we have proposed a new method to identify the MIMO channels for the single carrier zero padding block transmission system using optimal designed periodic precoding which minimize the noise effect in the estimation of the covariance matrix $\mathbf{R}_f$. With zero padding, the computation of the channel product matrix $\mathbf{HH}^*$ becomes particularly simple, since it amounts to solving a lower-triangular linear system. The channel impulse response matrix $\mathbf{H}$ is then computed, up to a unitary matrix ambiguity, from the channel product matrix via an eigen-decomposition. We summarize the proposed method as the following algorithm:
1) Select the optimal precoding sequence $p(n)$ given by (3.24), and form $\mathbf{G}_0^{-1}$ as in (3.29).
2) Collect the received data as $\bar{\mathbf{x}}(i)$ and pick up the first $(L+1)$ block entries of $\bar{\mathbf{x}}(i)$ as $\mathbf{x}_f(i)$. Then estimate the covariance matrix $\mathbf{R}_f$ via the time average

$$\hat{\mathbf{R}}_f = \frac{1}{S}\sum_{i=1}^{S} \mathbf{x}_f(i)\mathbf{x}_f(i)^*, \tag{3.30}$$

where S is the number of data block.
3) Compute $\widehat{\text{vec}(\mathbf{HH}^*)} = \mathbf{G}_0^{-1}\text{vec}(\hat{\mathbf{R}}_f)$ to obtain the elements of $\mathbf{HH}^*$.
4) Form the matrix $\mathbf{Q} = \mathbf{HH}^*$ and obtain the channel impulse response matrix by computing the K largest eigenvalues and the associated eigenvectors of $\mathbf{Q}$.

3.3 Channel Equalization

Once the received data $\bar{\mathbf{x}}(i) = \mathbf{H_e}\bar{\mathbf{s}}(i)+\bar{\mathbf{w}}(i)$ is available and the channel is identified, the minimum mean square error (MMSE) or zero forcing (ZF) equalization methods [13, 14] can be used to recover the modulated sources $s_k(n)$. For example, with an MMSE equalizer, $\mathbf{G}_\text{e}$, we estimate $\bar{\mathbf{s}}(i)$ by $\widehat{\bar{\mathbf{s}}}(i) = \mathbf{G}_\text{e}\bar{\mathbf{x}}(i)$. Since the precoding scheme is applied at the transmitter, we need to multiply the estimated $\bar{\mathbf{s}}(i)$ by $\mathbf{P}^{-1}$ to obtain an estimate of $\bar{\mathbf{v}}(i)$, where $\bar{\mathbf{v}}(i)$ is similarly defined as $\bar{\mathbf{s}}(i)$, and $\mathbf{P} = \mathbf{I}_{\frac{M}{L+1}} \otimes (\text{diag}[p(0), \cdots, p(L)] \otimes \mathbf{I}_K)$. In other words, the estimated $\bar{\mathbf{v}}(i)$ can be obtained by

$$\widehat{\bar{\mathbf{v}}}(i) = \mathbf{P}^{-1}\mathbf{G}_\text{e}\bar{\mathbf{x}}(i). \tag{3.31}$$

From (3.31), we know the equalization performance is related to $\mathbf{P}^{-1}$ and $\mathbf{G}_\text{e}$. Because $\mathbf{G}_\text{e}$ is formed from the estimated channel coefficients, we expect good channel identification to bring an accurate $\mathbf{G}_\text{e}$ and thus improves the equalization performance. Also we know using the optimal precoding sequence in (3.24), the identification performance improves as τ

decreases. Hence using a small τ brings good channel estimation and improves the accuracy of $\mathbf{G}_{\rm e}$, which is expected to improves the equalization performance. However, using a small τ would make the diagonal gain $p(k)^{-1} = \frac{1}{\sqrt{\tau}}$ in $\mathbf{P}^{-1}$, $k = 1, 2, \cdots, L$, becomes large, which results in large noise amplification at the receiver and hence is more likely to cause decision error. Therefore using a small τ would amplify the noise and the equalization performance deteriorates as τ decreases.

In summary, although decreasing τ improves the accuracy of $\mathbf{G}_{\rm e}$, it would cause an increased amplification of noise, and vice versa. Hence there is a trade-off on the selection of τ when channel equalization is performed. In the work of [15, 16, 27], this trade-off is also observed. We will give a simulation example to demonstrate this trade-off in the next section.

3.4 Simulation Results

In this section, we use several examples to demonstrate the performance of the proposed method. The channel NRMSE, SNR, and the number of Monte Carlo runs are the same as those given in Section 2.5. The source symbols are i.i.d. QPSK signals. The channel noise is zero mean, temporally and spatially white Gaussian.

1) Simulation 1 – optimal selection of precoding sequences

In this simulation, we use the model (2.33) to demonstrate the performance of the proposed method. The length of symbol blocks is $M = 27$, which is zero padded to blocks of length $M + P = 30$. It means $P = 3(= L + 1)$ and transmission efficiency is 90%. In experiment 1, we use 5 precoding sequences which all satisfy (3.20) and (3.21) to illustrate the effect of the precoding sequences on the identification performance. The first sequence S_0 are chosen based on (3.24) for $\tau = 0.6$, i.e., S_0 is chosen as $\{\sqrt{1.8}\ \sqrt{0.6}\ \sqrt{0.6}\}$. The sequences S_1, S_2, $\mathrm{S}_{\rm A}$, and $\mathrm{S}_{\rm B}$ are chosen as $\{\sqrt{0.6}\ \sqrt{1.8}\ \sqrt{0.6}\}$, $\{\sqrt{0.6}\ \sqrt{0.6}\ \sqrt{1.8}\}$, $\{\sqrt{0.6}\ \sqrt{1.0}\ \sqrt{1.4}\}$, and $\{1\ 1\ 1\}$ (i.e., no precoding), respectively. Figure 3.2 shows that for SNR=10 dB, the NRMSE decreases as the number of symbol blocks increases for every precoding sequence. As expected, the optimal precoding sequence S_0 yields the smallest NRMSE.

In experiment 2, we use the precoding sequences that satisfy (3.24), but with different τ to test the effect of τ on the identification performance. Figure 3.3 shows that when the number of symbol blocks = 100, the NRMSE decreases as SNR increases and is roughly constant for SNR $\geq$ 20 dB for different τ. Figures 3.3 also shows that the identification performs better for smaller τ.

2) Simulation 2 – channel order overestimation

In this simulation, we use the channel model (2.33) with SNR = 10 dB, fix the number of symbol blocks at 300, and use the precoding sequence that satisfies (3.24) with $\tau = 0.6$. For each upper bound $\hat{L}$, $0 \leq (\hat{L} - L) \leq 6$, we choose $P = \hat{L} + 1$ and $M = 9P$ for simulation such that the transmission efficiency is maintained at 90%. Figure 3.4 shows the NRMSE increases with increasing channel order overestimation for each τ. We see that periodic precoding improves robustness to channel order overestimation. For example, without precoding ($\tau = 1$), the NRMSE increases about 6 dB for $(\hat{L} - L) = 3$. With precoding, ($\tau = 0.4$), the corresponding increase in NRMSE is about 1.5 dB.

3) Simulation 3 – a 3-input 2-output channel

In this simulation, we use the 3-input 2-output model (2.35) to illustrate the performance of the proposed method for channel with more transmitters than receivers. We use $M = 27$ and $P = 3$. In experiment 1, we use the same precoding sequences S_0, S_1, and S_2 which are used in simulation 1. Figure 3.5 shows that for SNR=10 dB, the NRMSE decreases as the number of symbol blocks increases for each precoding sequence. The optimal precoding sequence S_0 yields the smallest NRMSE.

In experiment 2, we use the precoding sequences that satisfy (3.24), but with different τ to test the effect of τ on the identification performance. Figure 3.6 shows that the channel NRMSE decreases as SNR increases for each τ and that the identification method performs better for smaller τ.

4) Simulation 4 – trade-off in selecting τ

In this simulation, we discuss the trade-off in selecting τ when channel equalization is performed. We use the MMSE equalizer [13, 14]. We generate 150 2-input 2-output complex random channels based on the IEEE 802.11a standard [36, p. 336]. The sampling frequency is 20 MHZ and the the delay spread is 35 nsec (for home environment). Thus the orders of the channels are $L = 7$. We use M=56 and $P = L + 1 = 8$ such that $N = M + P = 64$. The number of symbol blocks is 250. We use the optimal precoding sequences which satisfy (3.24) with various τ.

Figure 3.7 shows that the identification performs better for smaller τ. Figure 3.8(a) shows that for $\tau \in [0.1, 0.8]$, the bit error rate (BER) performance deteriorates as τ decreases and the BER for $\tau = 0.7$ and $\tau = 0.8$ are very close. Figure 3.8(b) shows that for large τ, $\tau \geq 0.8$, the BER performance improves as τ decreases. Figure 3.8 shows that there is a trade-off between identification accuracy and noise amplification: a small τ means large noise amplification and an accurate channel estimate, and vice versa. For this

example, it seems a τ between 0.7 and 0.8 is a good choice for BER performance.

5) Simulation 5 – comparison with the subspace method

In this simulation, we again generate 300 2-input 2-output channels based on IEEE 802.11a standard. We use the precoding sequences that satisfy (3.24) with $\tau = 0.8$. We use Gray-coded QPSK and 16-QAM input symbols for simulation. We compare the identification and MMSE equalization performances of the proposed method with those of the subspace method [26] for MIMO SC-ZP systems.

Figure 3.9(a) shows that when the number of symbol blocks is 200, the identification performance of the proposed method is better than that of the subspace method except SNR $>$ 16 dB. The proposed method yields almost the same identification performance for QPSK and 16-QAM input symbols. Figure 3.9(b) shows that the equalization performance of the proposed method is better than that of the subspace method except SNR $>$ 16 dB. Figure 3.9 shows that the identification and equalization performance of the proposed method is better than those of the subspace method for low to medium SNR. The subspace method gives smaller BER than the proposed method for SNR$>$ 16 dB.

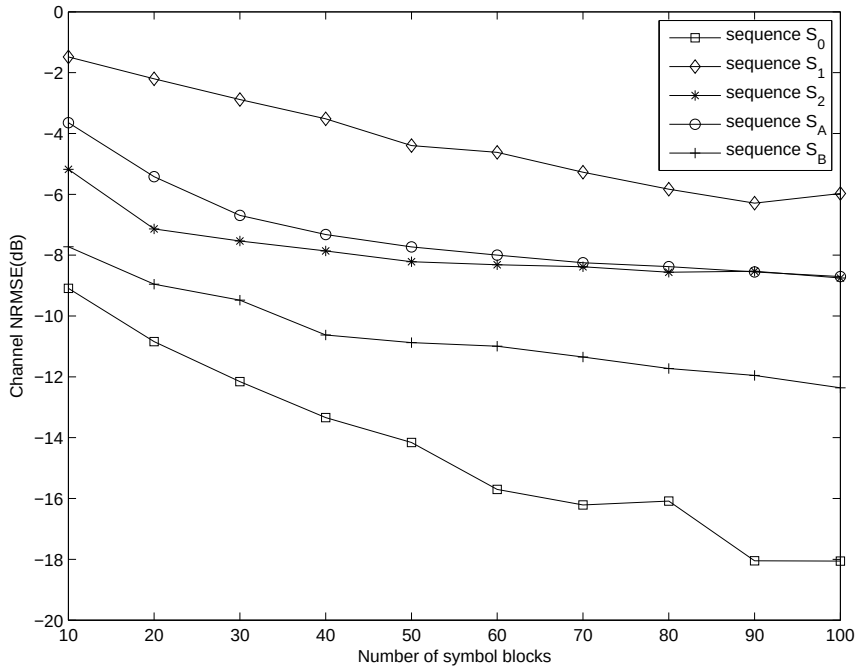

Figure 3.2. Channel NRMSE versus number of symbol blocks

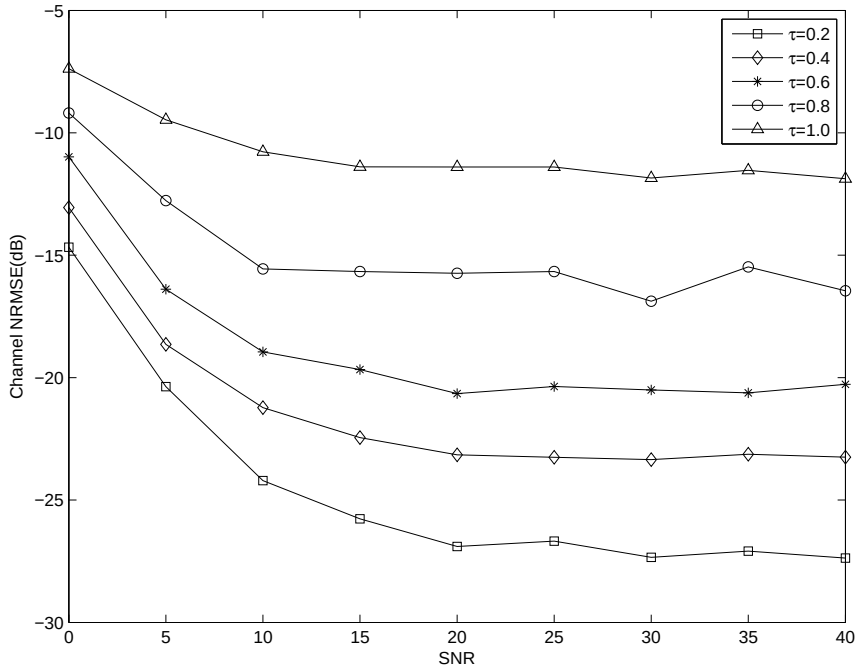

Figure 3.3. Channel NRMSE versus output SNR

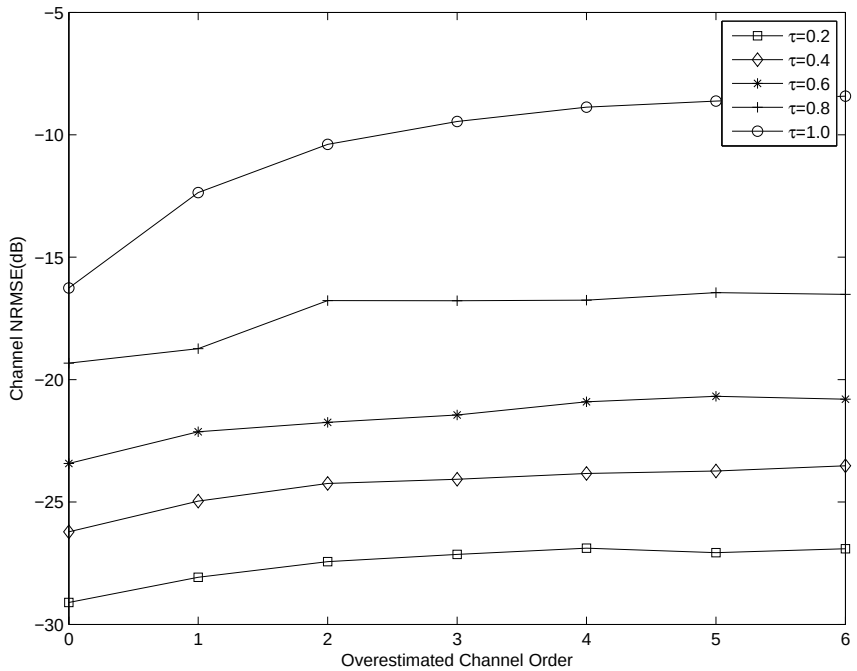

Figure 3.4. Channel NRMSE versus $(\hat{L} - L)$

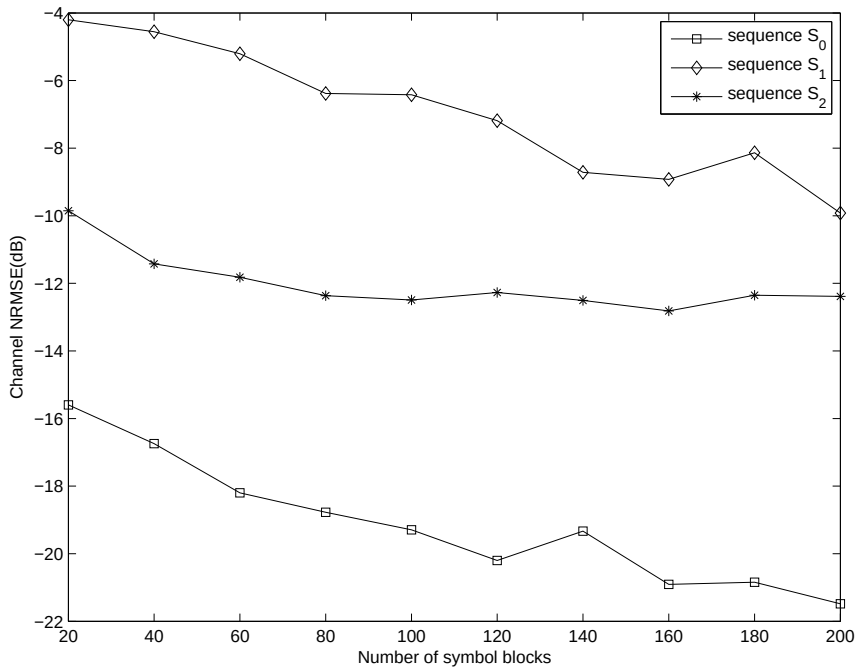

Figure 3.5. Channel NRMSE versus number of symbol blocks

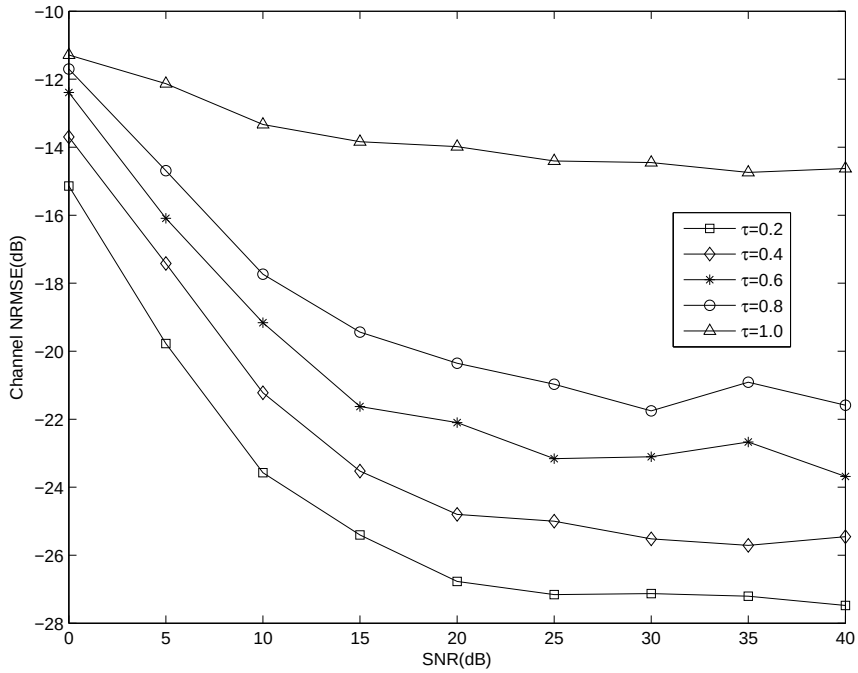

Figure 3.6. Channel NRMSE versus output SNR

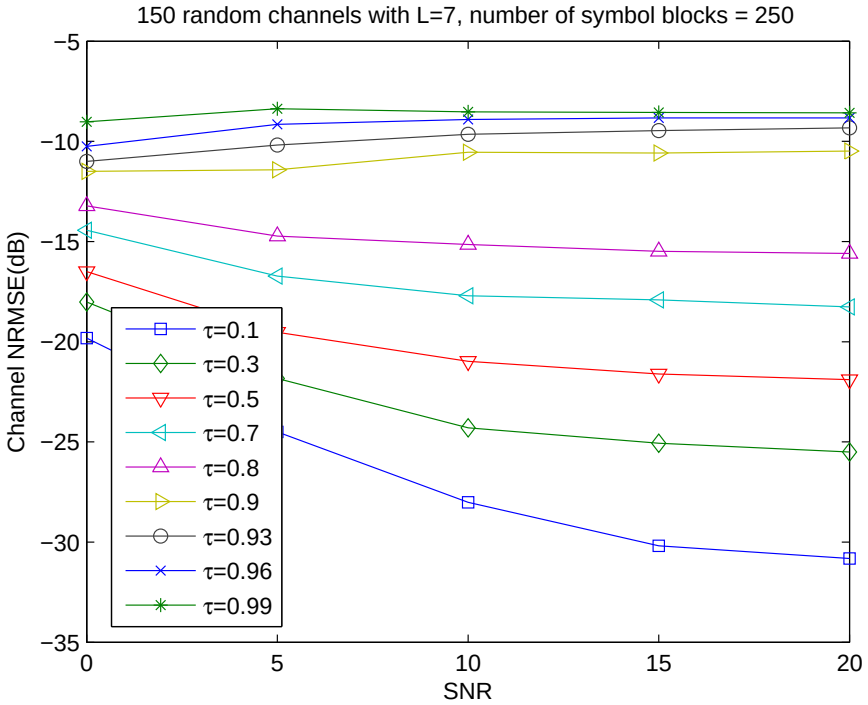

Figure 3.7. Channel NRMSE versus output SNR

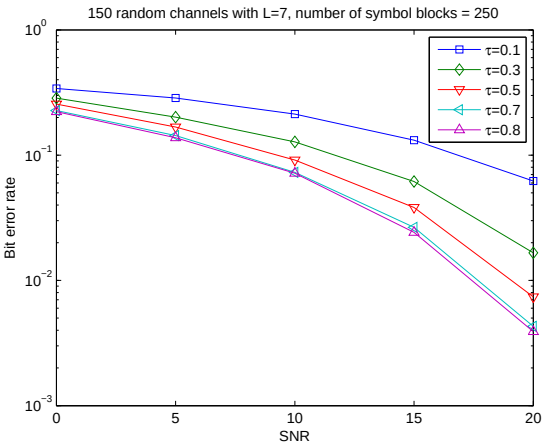

(a)

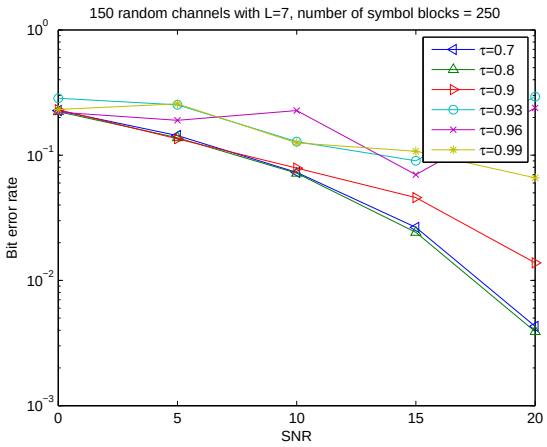

(b)

Figure 3.8. BER versus output SNR

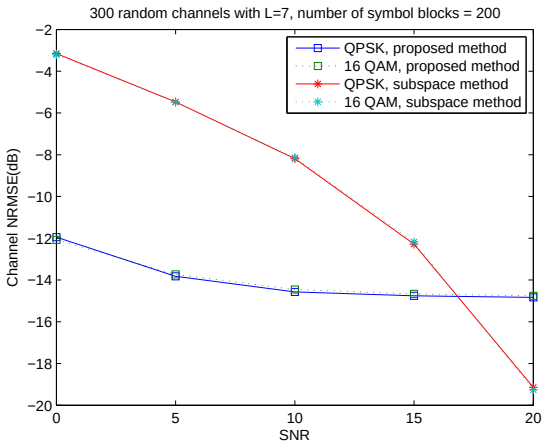

(a) Channel NRMSE versus output SNR

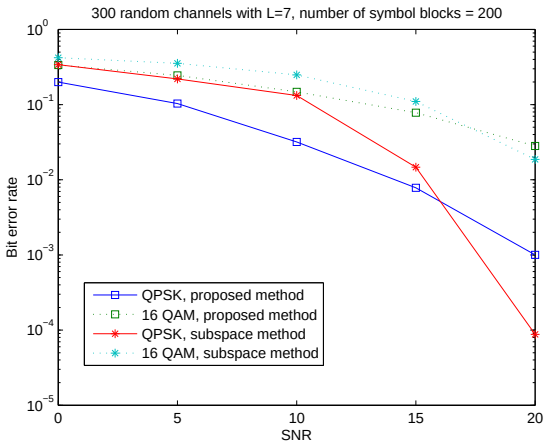

(b) Bit error rate versus output SNR

Figure 3.9. Comparison with the subspace method

Chapter 4

A Simplified Identification Algorithm for MIMO Zero Padding Channels

In this chapter, we propose a simplified identification method for MIMO SC-ZP block transmission systems without periodic precoding. The proposed method can also apply to MIMO ZP-OFDM systems. With zero-padding, the relation between the covariance matrix of the received data and the channel product matrices becomes highly structured. The structure makes it easy to estimate the channel product matrices and the noise covariance matrices. Eigen-decomposition of a Hermitian matrix formed by the channel product matrices yields the channel impulse response up to a unitary matrix ambiguity. The proposed method is shown to be robust to channel order overestimation. The channel noise may be temporally and spatially colored, the channel needs not be irreducible or column reduced, and there can be more outputs or more inputs. Simulation results are used to demonstrate the performance of the proposed method.

4.1 System Model and Formulation

Consider the K-input J-output discrete time SC-ZP block transmission baseband model shown in Figure 4.1. Following the same derivation process in Section 3.1, we have the relation of block inputs and outputs as follows.

$$\bar{\mathbf{x}}(i) = \mathbf{H_0}\bar{\mathbf{u}}(i) + \mathbf{H_1}\bar{\mathbf{u}}(i-1) + \bar{\mathbf{w}}(i), \tag{4.1}$$

where $\bar{\mathbf{u}}(i)$, $\bar{\mathbf{w}}(i)$, $\bar{\mathbf{x}}(i)$, $\mathbf{H_0}$ and $\mathbf{H_1}$ are those defined in Section 3.1. In addition, we make the following assumptions.

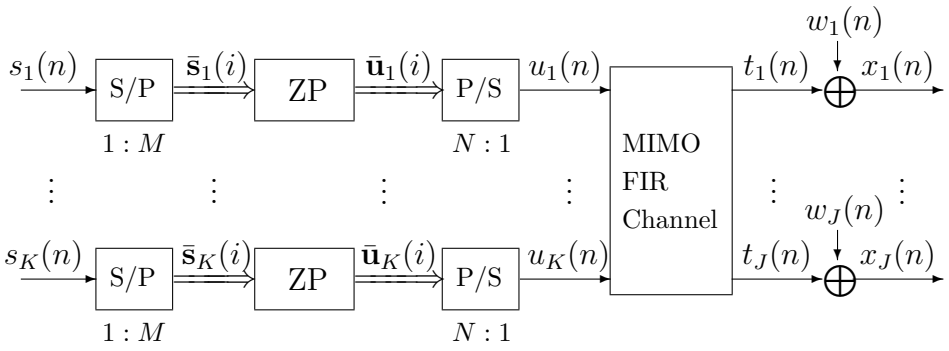

Figure 4.1. An MIMO single carrier with zero padding block transmission baseband model

(C1) The source signal $\mathbf{s}(n) = [s_1(n)\ s_2(n)\ \cdots\ s_K(n)]^T \in \mathbb{C}^K$ is a zero mean white sequence with $E[\mathbf{s}(m)\mathbf{s}(n)^*] = \delta(m-n)\mathbf{I}_K \in \mathbb{R}^{K\times K}$, where $\delta(\cdot)$ is the Kronecker delta function. The noise is zero mean, wide-sense stationary, and may be temporally and spatially colored with $E[\mathbf{w}(m)\mathbf{w}(m+d)^*] = \mathbf{K}_{\mathbf{w}}(d) \in \mathbb{C}^{J\times J}$. In addition, the source signal is uncorrelated with the noise $\mathbf{w}(n)$, i.e., $E[\mathbf{s}(m)\mathbf{w}(n)^*] = \mathbf{0}_{K\times J}$, $\forall\, m, n$.

(C2) An upper bound $\hat{L}$ of the channel order L is known, $P = \hat{L} + 1$, and $M > P$.

(C3) The channel impulse response matrix $\mathbf{H} = [\mathbf{H}(0)^T\ \mathbf{H}(1)^T \cdots \mathbf{H}(L)^T]^T$ is full column rank, i.e., rank($\mathbf{H}$)=K.

In the next section, we propose an algorithm for blind identification of the MIMO channel impulse response matrix $\mathbf{H}$ using second-order statistics of the received data.

4.2 Blind Channel Identification

In this section, we derive the proposed method under assumptions (**C1**), (**C2**), and (**C3**). Application of the proposed method to MIMO ZP-OFDM systems is given in Section 4.3.

4.2.1 The Identification Method

We first derive the proposed method for the case where the channel order L is known with $P = L + 1$, and there are more receivers, i.e., $J \geq K$. The cases of channel order

overestimation and more transmitters than receivers (i.e., $K > J$) are given at the end of this sub-section.

Due to assumption (**C2**) and the effect of zero padding, we know (4.1) can be expressed in a simple form $\bar{\mathbf{x}}(i) = \mathbf{H_0}\bar{\mathbf{u}}(i) + \bar{\mathbf{w}}(i)$ shown as follows:

$$\overbrace{\begin{bmatrix} \mathbf{x}(iN) \\ \vdots \\ \mathbf{x}(iN+L) \\ \vdots \\ \mathbf{x}(iN+M-1) \\ \vdots \\ \mathbf{x}(iN+N-1) \end{bmatrix}}^{\bar{\mathbf{x}}(i)} = \overbrace{\begin{bmatrix} \mathbf{H}(0) & & & & \\ \vdots & \ddots & & & \\ \mathbf{H}(L) & \cdots & \mathbf{H}(0) & & \\ & \ddots & \vdots & \ddots & \\ & & \mathbf{H}(L) & \cdots & \mathbf{H}(0) \\ & & & \ddots & \vdots \\ & & & & \underbrace{\mathbf{H}(L) \cdots \mathbf{H}(0)}_{(L+1)\ blocks} \end{bmatrix}}^{\mathbf{H_0}} \overbrace{\begin{bmatrix} \mathbf{u}(iN) \\ \vdots \\ \mathbf{u}(iN+L) \\ \vdots \\ \mathbf{u}(iN+M-1) \\ \mathbf{0} \\ \vdots \\ \mathbf{0} \end{bmatrix}}^{\bar{\mathbf{u}}(i)} + \bar{\mathbf{w}}(i). \tag{4.2}$$

Let $\mathbf{x}_f(i) = [\mathbf{x}(iN)^T \ \cdots \ \mathbf{x}(iN+L)^T]^T$ be the first $(L+1)$ block rows of $\bar{\mathbf{x}}(i)$. Then

$$\mathbf{x}_f(i) = \mathbf{H}_f\mathbf{u}_f(i) + \mathbf{w}_f(i), \tag{4.3}$$

where $\mathbf{H}_f \in \mathbb{C}^{J(L+1)\times K(L+1)}$ is the sub-matrix formed by the first $(L+1)$ block columns and block rows of $\mathbf{H}_0$, and $\mathbf{u}_f(i)$, $\mathbf{w}_f(i)$ are similarly defined as $\mathbf{x}_f(i)$. Taking expectation of $\mathbf{x}_f(i)\mathbf{x}_f(i)^*$, we get

$$\mathbf{R}_f = E[\mathbf{x}_f(i)\mathbf{x}_f(i)^*] = \mathbf{H}_f\mathbf{H}_f^* + \mathbf{K}_f, \tag{4.4}$$

where $\mathbf{K}_f$ is a Hermitian and block Toeplitz matrix and each block on the jth block super-diagonal is equal to $\mathbf{K_w}(j)$ for $j = 0, 1, \cdots, L$. Since $\mathbf{H}_f$ is block lower triangular, we have

$$\begin{cases} \Upsilon_0(\mathbf{R}_f) = [\mathbf{H}(0)\mathbf{H}(0)^* + \mathbf{K_w}(0) & \sum_{l=0}^{1}\mathbf{H}(l)\mathbf{H}(l)^* + \mathbf{K_w}(0) & \cdots & \sum_{l=0}^{L}\mathbf{H}(l)\mathbf{H}(l)^* + \mathbf{K_w}(0)] \\ \Upsilon_1(\mathbf{R}_f) = [\mathbf{H}(0)\mathbf{H}(1)^* + \mathbf{K_w}(1) & \sum_{l=0}^{1}\mathbf{H}(l)\mathbf{H}(l+1)^* + \mathbf{K_w}(1) & \cdots & \sum_{l=0}^{L-1}\mathbf{H}(l)\mathbf{H}(l+1)^* + \mathbf{K_w}(1)] \\ \Upsilon_2(\mathbf{R}_f) = [\mathbf{H}(0)\mathbf{H}(2)^* + \mathbf{K_w}(2) & \sum_{l=0}^{1}\mathbf{H}(l)\mathbf{H}(l+2)^* + \mathbf{K_w}(2) & \cdots & \sum_{l=0}^{L-2}\mathbf{H}(l)\mathbf{H}(l+2)^* + \mathbf{K_w}(2)] \\ \quad\vdots \quad\quad \vdots & \vdots & & \\ \Upsilon_{L-1}(\mathbf{R}_f) = [\mathbf{H}(0)\mathbf{H}(L-1)^* + \mathbf{K_w}(L-1) & \sum_{l=0}^{1}\mathbf{H}(l)\mathbf{H}(l+L-1)^* + \mathbf{K_w}(L-1)] & & \\ \Upsilon_L(\mathbf{R}_f) = [\mathbf{H}(0)\mathbf{H}(L)^* + \mathbf{K_w}(L)]. & & & \end{cases} \tag{4.5}$$

Then for each $\Upsilon_j(\mathbf{R}_f)$, $j = 0, 1, \cdots, L$, keep the first block matrix and subtract the mth block matrix from the $(m+1)$th block matrix of $\Upsilon_j(\mathbf{R}_f)$, $m = 1, 2, \cdots, L-j \geq 1$. In this

way, we obtain the following matrices.

$$\begin{cases} \mathbf{E}_0 = [\mathbf{H}(0)\mathbf{H}(0)^* + \mathbf{K}_\mathbf{w}(0) & \mathbf{H}(1)\mathbf{H}(1)^* & \mathbf{H}(2)\mathbf{H}(2)^* & \cdots & \mathbf{H}(L)\mathbf{H}(L)^*] \\ \mathbf{E}_1 = [\mathbf{H}(0)\mathbf{H}(1)^* + \mathbf{K}_\mathbf{w}(1) & \mathbf{H}(1)\mathbf{H}(2)^* & \mathbf{H}(2)\mathbf{H}(3)^* & \cdots & \mathbf{H}(L-1)\mathbf{H}(L)^*] \\ \mathbf{E}_2 = [\mathbf{H}(0)\mathbf{H}(2)^* + \mathbf{K}_\mathbf{w}(2) & \mathbf{H}(1)\mathbf{H}(3)^* & \mathbf{H}(2)\mathbf{H}(4)^* & \cdots & \mathbf{H}(L-2)\mathbf{H}(L)^*] \\ \quad \vdots \quad \vdots & & \vdots & & \\ \mathbf{E}_{L-1} = [\mathbf{H}(0)\mathbf{H}(L-1)^* + \mathbf{K}_\mathbf{w}(L-1) & \mathbf{H}(1)\mathbf{H}(L)^*] & & & \\ \mathbf{E}_L = [\mathbf{H}(0)\mathbf{H}(L)^* + \mathbf{K}_\mathbf{w}(L)] & & & & \end{cases} \tag{4.6}$$

From (4.6), we can obtain the channel product matrices $\mathbf{H}(m)\mathbf{H}(n)^*$ for $m, n = 1, 2, \cdots, L$. If we can further obtain $\mathbf{H}(0)\mathbf{H}(j)^*$ for $j = 0, 1, \cdots, L$, then we can get a Hermitian matrix $\mathbf{Q} = \mathbf{H}\mathbf{H}^*$ formed by these channel product matrices. Similarly, under the assumption (**C3**), we can obtain the channel impulse response matrix, up to a unitary matrix ambiguity, by choosing the K largest eigenvalues and the associated eigenvectors of $\mathbf{Q}$, like the way given at the end of Section 2.2.1

Now, to obtain $\mathbf{H}(0)\mathbf{H}(j)^*$ for $j = 0, 1, \cdots, L$, we need to eliminate the noise covariance matrix imposing on $\mathbf{H}(0)\mathbf{H}(j)^* + \mathbf{K}_\mathbf{w}(j)$. We will take advantage of the special structure of the last P block entries of $\bar{\mathbf{x}}(i)$, i.e., $\mathbf{x}_l = [\mathbf{x}(iN+M)^T \ \cdots \ \mathbf{x}(iN+N-1)^T]^T$ to eliminate $\mathbf{K}_\mathbf{w}(j)$ for $j = 0, 1, \cdots, L$.

From (4.2), we know $\mathbf{x}_l(i)$ can be written as

$$\overbrace{\begin{bmatrix} \mathbf{x}(iN+M) \\ \mathbf{x}(iN+M+1) \\ \vdots \\ \mathbf{x}(iN+N-1) \end{bmatrix}}^{\mathbf{x}_l(i)} = \overbrace{\begin{bmatrix} \mathbf{0}\cdots\mathbf{0} & \mathbf{H}(L) & \cdots & \mathbf{H}(1) & \mathbf{H}(0) & & \\ & \mathbf{H}(L) & \cdots & \mathbf{H}(1) & \mathbf{H}(0) & & \\ & & \ddots & \ddots & \ddots & & \\ & & & \underbrace{\mathbf{0}}_{M \ blocks} & \underbrace{\mathbf{H}(L)\cdots\mathbf{H}(1)}_{P(=L+1) \ blocks} & \mathbf{H}(0) & \end{bmatrix}}^{\mathbf{H}_l} \overbrace{\begin{bmatrix} \mathbf{u}(iN) \\ \vdots \\ \mathbf{u}(iN+M-1) \\ \mathbf{0} \\ \vdots \\ \mathbf{0} \end{bmatrix}}^{\bar{\mathbf{u}}(i)} + \mathbf{w}_l(i), \tag{4.7}$$

where $\mathbf{w}_l(i)$ is similarly defined as $\mathbf{x}_l(i)$. Because the last P block rows in $\bar{\mathbf{u}}(i)$ are zero and $P = L + 1$, $\mathbf{x}_l(i)$ can be written as

$$\mathbf{x}_l(i) = \mathbf{H}_r[\mathbf{u}(iN)^T \ \cdots \ \mathbf{u}(iN+M-1)^T]^T + \mathbf{w}_l(i) = \mathbf{H}_r\mathbf{u}_r(i) + \mathbf{w}_l(i), \tag{4.8}$$

where $\mathbf{H}_r$, the first M block columns of $\mathbf{H}_l$, is a $JP \times KM$ block Toeplitz matrix with the first block row being $[\underbrace{\mathbf{0}_{J\times K}\cdots\mathbf{0}_{J\times K}}_{(M-L) \ blocks} \ \mathbf{H}(L) \ \mathbf{H}(L-1) \ \cdots \ \mathbf{H}(1)]$ and the first block column being zero, as seen from (4.7). Let $\mathbf{R}_l = E[\mathbf{x}(iN+M)\mathbf{x}_l^*(i)]$. Then from (4.7) and (4.8),

we have

$$\begin{aligned}\mathbf{R}_l &= [E[\mathbf{x}(iN+M)\mathbf{x}(iN+M)^*] \;\; E[\mathbf{x}(iN+M)\mathbf{x}(iN+M+1)^*] \;\; \cdots \;\; E[\mathbf{x}(iN+M)\mathbf{x}(iN+N-1)^*]] \\ &= [\underbrace{\sum_{l=1}^{L}\mathbf{H}(l)\mathbf{H}(l)^* + \mathbf{K}_{\mathbf{w}}(0)}_{\mathbf{R}_l(0)} \;\; \underbrace{\sum_{l=1}^{L-1}\mathbf{H}(l)\mathbf{H}(l+1)^* + \mathbf{K}_{\mathbf{w}}(1)}_{\mathbf{R}_l(1)} \;\; \cdots \;\; \underbrace{\mathbf{K}_{\mathbf{w}}(L)}_{\mathbf{R}_l(L)}].\end{aligned} \tag{4.9}$$

From (4.5), the last block column (in reverse order) of $\mathbf{R}_f$ gives the matrix $\mathbf{R}_m$:

$$\mathbf{R}_m = [\underbrace{\sum_{l=0}^{L}\mathbf{H}(l)\mathbf{H}(l)^* + \mathbf{K}_{\mathbf{w}}(0)}_{\mathbf{R}_m(0)} \;\; \underbrace{\sum_{m=0}^{L-1}\mathbf{H}(l)\mathbf{H}(l+1)^* + \mathbf{K}_{\mathbf{w}}(1)}_{\mathbf{R}_m(1)} \;\; \cdots \;\; \underbrace{\mathbf{H}(0)\mathbf{H}(L)^* + \mathbf{K}_{\mathbf{w}}(L)}_{\mathbf{R}_m(L)}], \tag{4.10}$$

where $\mathbf{R}_l(i)$ and $\mathbf{R}_m(i) \in \mathbb{C}^{J\times J}$ for $i = 0, 1, \cdots, L$. Then subtracting (4.9) from (4.10), we can obtain the channel product matrices $\mathbf{H}(0)\mathbf{H}(0)^*$, $\mathbf{H}(0)\mathbf{H}(1)^*$, $\cdots$, $\mathbf{H}(0)\mathbf{H}(L)^*$. The noise covariance matrix $\mathbf{K}_{\mathbf{w}}(j)$ for $j = 0, 1, \cdots, L$ can also be obtained. Hence we can form the Hermitian matrix $\mathbf{Q} = \mathbf{H}\mathbf{H}^*$ and estimate the channel impulse response matrix $\mathbf{H}$ by taking eigen-decomposition of $\mathbf{Q}$.

Remark 1: If we choose $P = L$ instead of $P = L+1$, $\mathbf{H_1}\bar{\mathbf{u}}(i-1) = \mathbf{0}$ in (4.1) still holds and we can also obtain (4.6). However, we can not eliminate the noise covariance matrix imposing on $\mathbf{H}(0)\mathbf{H}(L)^* + \mathbf{K}_{\mathbf{w}}(L)$. More precisely, when $P = L$, then (4.9) and (4.10) will become $\mathbf{R}_l(1:J, 1:J\times L) = [\mathbf{R}_l(0) \;\; \mathbf{R}_l(1) \;\; \cdots \;\; \mathbf{R}_l(L-1)]$ and $\mathbf{R}_m(1:J, 1:J\times L) = [\mathbf{R}_m(0) \;\; \mathbf{R}_m(1) \;\; \cdots \;\; \mathbf{R}_m(L-1)]$, respectively. The difference of these two matrices gives $\mathbf{H}(0)\mathbf{H}(0)^*, \mathbf{H}(0)\mathbf{H}(1)^*, \cdots, \mathbf{H}(0)\mathbf{H}(L-1)^*$. The remaining unknown is $\mathbf{H}(0)\mathbf{H}(L)^*$. Thus we need to use $P = L+1$ when $\mathbf{K}_{\mathbf{w}}(L) \neq \mathbf{0}$. However, if $\mathbf{K}_{\mathbf{w}}(L) = \mathbf{0}$, e.g., temporally white noise case ($\mathbf{K}_{\mathbf{w}}(j) = \mathbf{0}$ for $j = 1, 2, \cdots, L$), we choose $P = L$ because we can directly obtain $\mathbf{H}(0)\mathbf{H}(L)^*$ from $\mathbf{E}_L$ in (4.6).

Remark 2: So far we have assumed that the channel order L is known. If only an upper bound $\hat{L} \geq L$ is available (in this case, assumption (**C2**) becomes: $M > P$, $P = \hat{L}+1$), then following the same process given in this sub-section , we observe that (4.6) becomes $\widehat{\mathbf{E}}_j = [\mathbf{E}_j \;\; \underbrace{\mathbf{0}_{J\times J} \;\; \cdots \;\; \mathbf{0}_{J\times J}}_{(\hat{L}-L)\;\; blocks}]$ for $j = 0, 1, \cdots, L$ and $\widehat{\mathbf{E}}_j = [\underbrace{\mathbf{K}_{\mathbf{w}}(j) \;\; \mathbf{0}_{J\times J} \;\; \cdots \;\; \mathbf{0}_{J\times J}}_{(\hat{L}-j)\;\; blocks}]$ for $j = L+1, L+2, \cdots, \hat{L}$. Then after noise covariance matrices elimination, we can also obtain $\mathbf{Q}$ with the last $(\hat{L}-L)$ block columns and block rows being zero. Then similar to the discussion in Section 2.2.2, we can also identify the channel impulse response matrix.

Remark 3: The proposed method can apply to the case of more transmitters than receivers. Please see Section 2.2.3.

4.2.2 Identification Algorithm

So far, we have proposed a blind identification method for MIMO zero padding block transmission systems based on eigen-decomposition approach. With zero-padding, the relation between the covariance matrix of the received data and the channel product matrices becomes highly structured. The structure makes it easy to estimate the channel product matrices and the noise covariance matrices. Eigen-decomposition of a Hermitian matrix formed by the channel product matrices yields the channel impulse response up to a unitary matrix ambiguity. The channel noise may be temporally and spatially colored. We summarize the proposed method as the following algorithm.

Algorithm :

1) Collect the received data as $\bar{\mathbf{x}}(i)$, pick up the first $(L+1)$ block entries of $\bar{\mathbf{x}}(i)$ as $\mathbf{x}_f(i)$ and the last P block entries of $\bar{\mathbf{x}}(i)$ as $\mathbf{x}_l(i)$.

2) Estimate the matrices $\mathbf{R}_f$ and $\mathbf{R}_l$ via the following time average

$$\hat{\mathbf{R}}_f = \frac{1}{S}\sum_{i=1}^{S} \mathbf{x}_f(i)\mathbf{x}_f(i)^*, \tag{4.11}$$

$$\hat{\mathbf{R}}_l = \frac{1}{S}\sum_{i=1}^{S} \mathbf{x}(iN+M)\mathbf{x}_l(i)^*, \tag{4.12}$$

where S is the number of data block, and $\mathbf{x}(iN+M)$ is the $(M+1)$th block entry of $\bar{\mathbf{x}}(i)$.

3) Form $\Upsilon_j(\hat{\mathbf{R}}_f)$ as in (4.5) and then obtain $\mathbf{H}(m)\mathbf{H}(n)^*$ for $m, n = 1, 2, \cdots, L$.

4) Form (4.10) from $\Upsilon_j(\hat{\mathbf{R}}_f)$, $j = 0, 1, \cdots, L$, and form (4.9) from $\hat{\mathbf{R}}_l$. Then obtain $\mathbf{H}(0)\mathbf{H}(j)^*$ for $j = 0, 1, \cdots, L$ by subtracting (4.9) from (4.10).

5) Form the matrix $\mathbf{Q} = \mathbf{H}\mathbf{H}^*$ using the channel product matrices, and obtain the channel impulse response matrix $\mathbf{H}$ by computing the K largest eigenvalues and the associated eigenvectors of $\mathbf{Q}$.

4.2.3 Extension to MIMO Zero-Padding OFDM Systems

The proposed method can be extended to the MIMO ZP-OFDM systems. In this case, at the transmitter, each $\bar{\mathbf{s}}_k(i)$ is multiplied by the IFFT matrix $\mathbf{F}^*$ before entering the zero padding block, $\mathbf{F}_1$ [26]. Here $\mathbf{F} \in \mathbb{C}^{M\times M}$ is an FFT matix. Thus we know the input to $\mathbf{F}_1$ is $\mathbf{F}^*\bar{\mathbf{s}}_k(i)$ for OFDM case. Since $\mathbf{F}$ is a unitary matix [**?**], $\bar{\mathbf{s}}_k(i)$ and $\mathbf{F}^*\bar{\mathbf{s}}_k(i)$ are both zero mean and have the same second-order statistics. Hence

$$E[\mathbf{F}^*\bar{\mathbf{s}}_k(m)] = \mathbf{0}, \;\; E[(\mathbf{F}^*\bar{\mathbf{s}}_k(m))(\mathbf{F}^*\bar{\mathbf{s}}_k(n))^*] = \delta(m-n)\mathbf{I}_M.$$

Hence the first and second-order statistics of $\mathbf{u}(n)$ for OFDM case are the same as those for single carrier case. Therefore, following the same method given in Section 4.2.1, we can identify the channel impulse response matrix for ZP-OFDM system.

Remark : At the receiver for ZP-OFDM system, each $\bar{\mathbf{x}}_j(i)$, $j = 1, 2, \cdots, J$, enters an overlap added matrix $\mathbf{F}_2$, an FFT matrix $\mathbf{F}$, and the parallel-to-serial block to yield output [26]. Here $\mathbf{F}_2 = [\mathbf{I}_M \ \mathbf{L}_a] \in \mathbb{R}^{M\times(M+P)}$ with $\mathbf{L}_a = [\mathbf{I}_P \ \mathbf{0}^T_{(M-P)\times P}]^T$. However, we only use the data $\bar{\mathbf{x}}(i)$, which is a permutation of $[\bar{\mathbf{x}}_1(i)^T \ \bar{\mathbf{x}}_2(i)^T \ \cdots \ \bar{\mathbf{x}}_J(i)^T]^T$, to identify the channel impulse response matrix.

4.3 Simulation Results

In this section, we use several examples to demonstrate the performance of the proposed method. The channel NRMSE and the number of Monte Carlo runs are the same as those given in Section 2.5. The input source symbols are i.i.d. QPSK signals. The signal-to-noise ratio (SNR) at the output is defined as SNR $= \frac{E[\|\mathbf{t}(n)\|_2^2]}{E[\|\mathbf{w}(n)\|_2^2]}$, where $\mathbf{t}(n) = [t_1(n) \ \cdots \ t_J(n)]^T$ is the signal component of the received signal (see Figure 4.1). Except Simulation 1, the channel noise is zero mean, temporally and spatially white Gaussian.

1) Simulation 1 – color noise case

In this simulation, we use the channel model (2.32) to demonstrate the performance of the proposed method when the channel noise is colored. The length of symbol blocks is $M = 27$, which is zero padded to blocks of length $M+P = 30$. It means $P = 3(= L+1)$ and transmission efficiency is 90%. The additive color noise $\mathbf{w}(n)$ is generated by passing a zero mean, unit variance, temporally and spatially white Gaussian vector sequence $\mathbf{w_v}(n) \in \mathbb{R}^2$ through an FIR filter $\mathbf{C}(z) = \mathbf{C}(0)+\mathbf{C}(1)z^{-1}+\mathbf{C}(2)z^{-2}$ whose output is $\mathbf{w}(n) = \mathbf{C}(z)\mathbf{w_v}(n)$, where

$$\mathbf{C}(0) = \begin{bmatrix} 0.283 + 0.181i & 0.185 + 0.115i \\ -0.135 + 0.192i & 0.136 + 0.235i \end{bmatrix}, \ \mathbf{C}(1) = \begin{bmatrix} 0.185 + 0.126i & 0.165 + 0.235i \\ -0.154 + 0.102i & 0.108 + 0.338i \end{bmatrix},$$

$$\mathbf{C}(2) = \begin{bmatrix} 0.089 + 0.181i & 0.089 + 0.235i \\ 0.089 + 0.126i & 0.108 + 0.159i \end{bmatrix}$$

In this case, $\mathbf{K_w}(0)$, $\mathbf{K_w}(1)$, and $\mathbf{K_w}(2)$ defined in assumption (**B**) are shown as follows:

$$\mathbf{K_w}(0) = \begin{bmatrix} 0.397 & 0.208 - 0.159i \\ 0.208 + 0.159i & 0.350 \end{bmatrix}, \ \mathbf{K_w}(1) = \begin{bmatrix} 0.242 - 0.067i & 0.121 - 0.120i \\ 0.171 + 0.101i & 0.199 + 0.011i \end{bmatrix},$$

$$\mathbf{K_w}(2) = \begin{bmatrix} 0.101 - 0.068i & 0.086 - 0.037i \\ 0.090 + 0.031i & 0.064 + 0.038i \end{bmatrix}$$

Figure 4.2(a) shows the NRMSE decreases as the number of symbol blocks increases. Figure 4.2(b) shows that the noise NRMSE also decreases as the number of symbol blocks increases, where the noise NRMSE is similarly defined as in (2.32) except $\mathbf{H}$ is replaced by $\mathbf{K} = [\mathbf{K}_{\mathbf{w}}(0)^T\ \mathbf{K}_{\mathbf{w}}(1)^T\ \mathbf{K}_{\mathbf{w}}(2)^T]^T$ and $\widehat{\mathbf{H}}^{(i)}$ is replaced by $\widehat{\mathbf{K}}^{(i)} = [\widehat{\mathbf{K}}_{\mathbf{w}}^{(i)}(0)^T\ \widehat{\mathbf{K}}_{\mathbf{w}}^{(i)}(1)^T\ \widehat{\mathbf{K}}_{\mathbf{w}}^{(i)}(2)^T]^T$.

2) Simulation 2 – random channels case

In this simulation, we generate 100 2-input 2-output random channels with order $L = 2$ to demonstrate the performance of the proposed method. Each element in the channel impulse response matrix is complex Gaussian distribution with zero mean and unit variance. We use $M = 18$ and $P = 2(= L)$ (transmission efficiency is 90%). Figure 4.3 shows for different number of symbol blocks, the NRMSE decreases as SNR increases and is roughly constant for SNR $\geq$ 20 dB.

3) Simulation 3 – a 3-input 2-output channel

In this simulation, we use the 3-input 2-output model (2.35) to illustrate the performance of the proposed method for channel with more inputs than outputs. We use $M = 18$ and $P = 2$. Figure 4.4 shows for different number of symbol blocks, the NRMSE decreases as SNR increases and is roughly constant for SNR $\geq$ 20 dB.

4) Simulation 4 – channel order overestimation

In this simulation, we use the channel model (2.34) to demonstrate the performance of the proposed method by comparing with the subspace method [26], which is also for MIMO zero padding block transmission systems. For each upper bound $\hat{L}$, $0 \leq (\hat{L} - L) \leq 6$, we choose $P = \hat{L}$ and $M = 9P$ for simulation such that the transmission efficiency is maintained at 90%. Figure 4.5 shows when the number of symbol blocks is fixed at 500, the NRMSE increases with increasing channel order overestimation for different SNR. When SNR=0 and 5 dB, the proposed method performs better than the subspace method. When SNR=10 dB, the subspace method performs better than the proposed method. Figures 4.5 shows that the proposed method is more robust to channel order overestimation than the subspace method when SNR is low.

5) Simulation 5 – channel estimation and equalization of a 2-input 2-output ZP-OFDM system

In this simulation, we use a ZP-OFDM system with the same channel model (2.34), and $M = 18$, $P = 2$. We compare the performance of the proposed method with that of the subspace method [26]. Figure 4.6(a) shows when SNR = 0 and 5 dB, the performance of

the proposed method is better than that of the subspace method. However, when SNR = 10 dB, the performance of the subspace method is better than that of the proposed method. Figure 4.6(b) shows when the number of blocks is 100 (300), the proposed method performs better than the subspace method when SNR below about 8 dB (6 dB). Figures 4.6(a) and 4.6(b) show that the proposed method has better performance than the subspace method under low SNR.

Figure 4.7 shows the simulation results for the zero forcing equalization of the proposed method and the subspace method. The number of symbol blocks is 500 (where the number of symbols = $18 \times 2 \times 500 = 18000$). We first identify the channel using the first 25, 50, 250, and 500 symbol blocks, respectively, and then do equalization. In each sub-figure of Figure 4.7, we see the proposed method performs better than the subspace method under low SNR, whereas the subspace method performs better under high SNR. Besides, from Figure 4.7, we can also observe the tendency that when the number of symbol blocks used for identification increases, the equalization performance of the proposed method and the subspace method would tend to be identical. Simulation result in Figure 4.8 shows when the number of symbol blocks for identification and equalization is 5000, the performance of these two methods are almost identical.

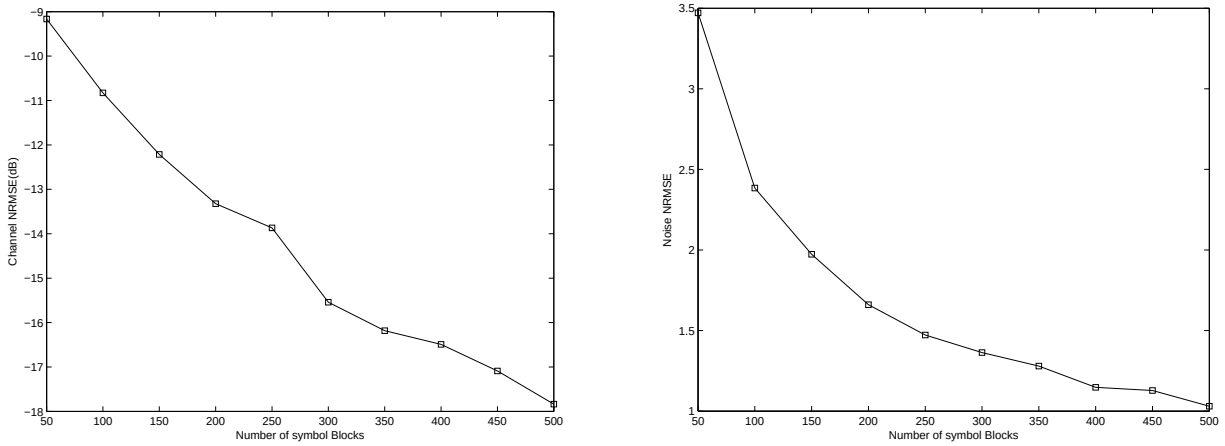

(a) Channel NRMSE versus number of symbol blocks

(b) Noise NRMSE versus number of symbol blocks

Figure 4.2. Color noise case

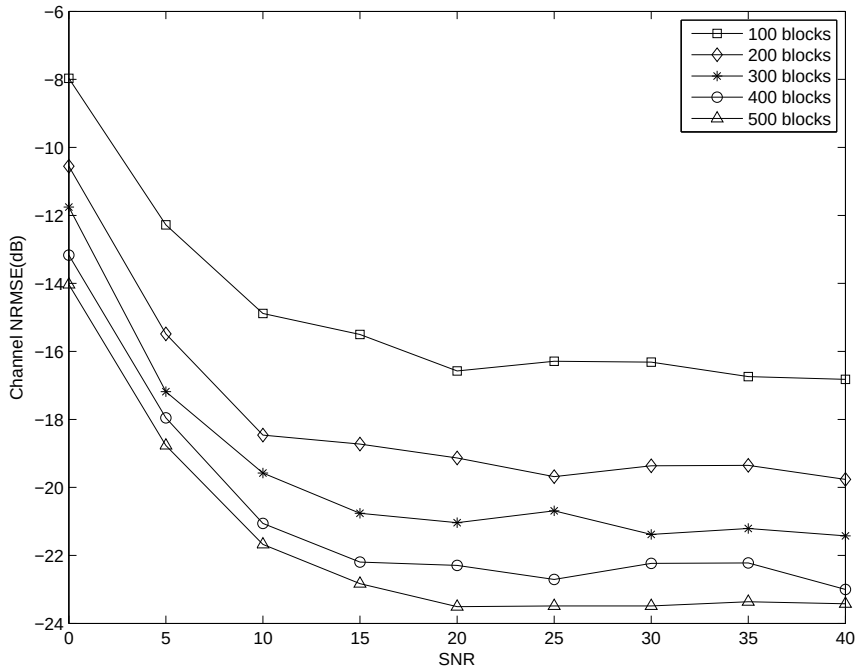

Figure 4.3. Channel NRMSE versus output SNR

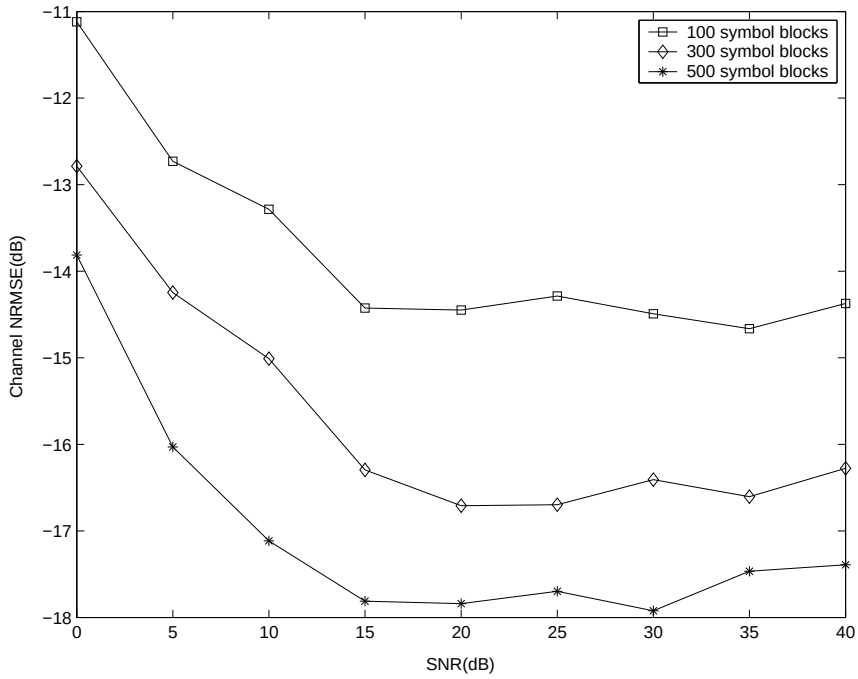

Figure 4.4. Channel NRMSE versus output SNR

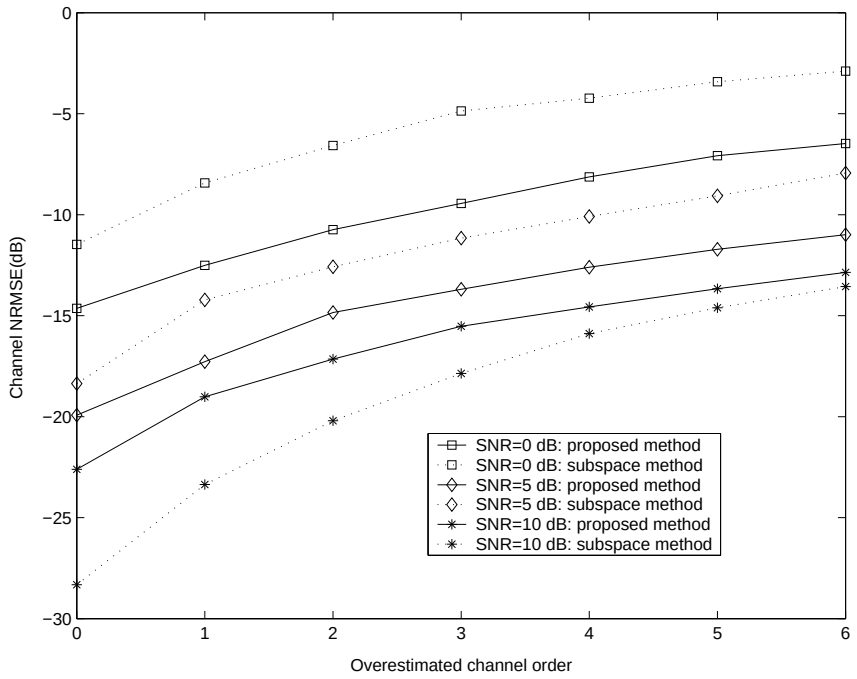

Figure 4.5. Channel NRMSE versus $(\hat{L} - L)$

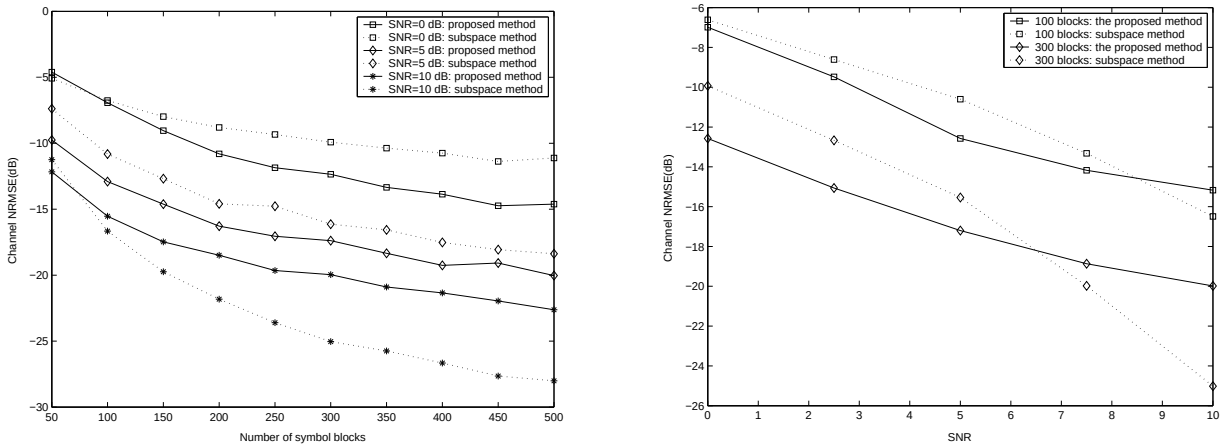

(a) Channel NRMSE versus number of symbol blocks

(b) Channel NRMSE versus output SNR

Figure 4.6. An OFDM system case

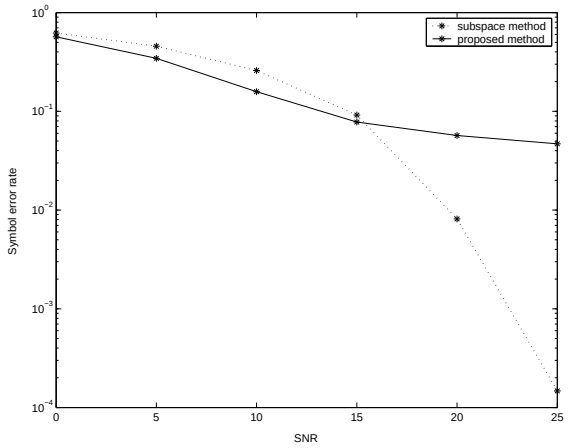

(a) 25 symbol blocks for identification

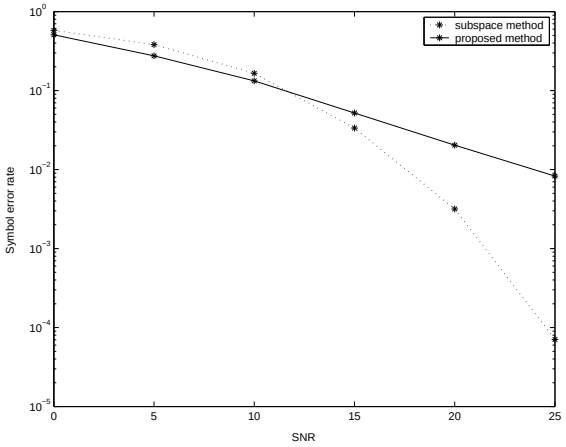

(b) 50 symbol blocks for identification

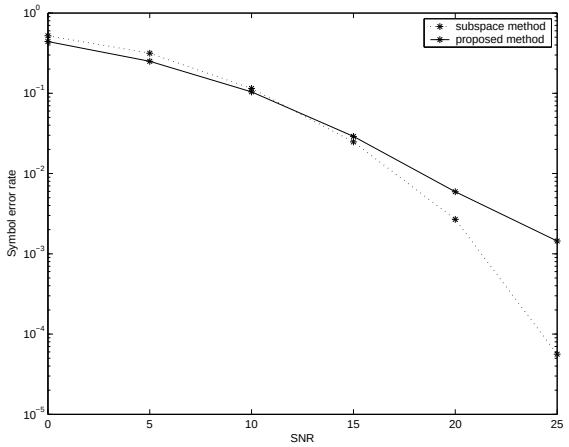

(c) 250 symbol blocks for identification

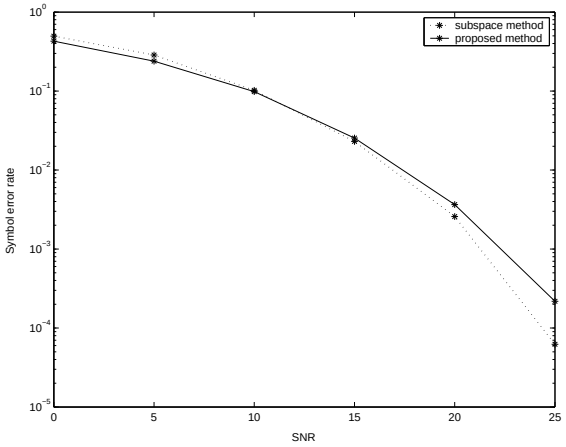

(d) 500 symbol blocks for identification

Figure 4.7. An OFDM system: symbol error rate versus output SNR

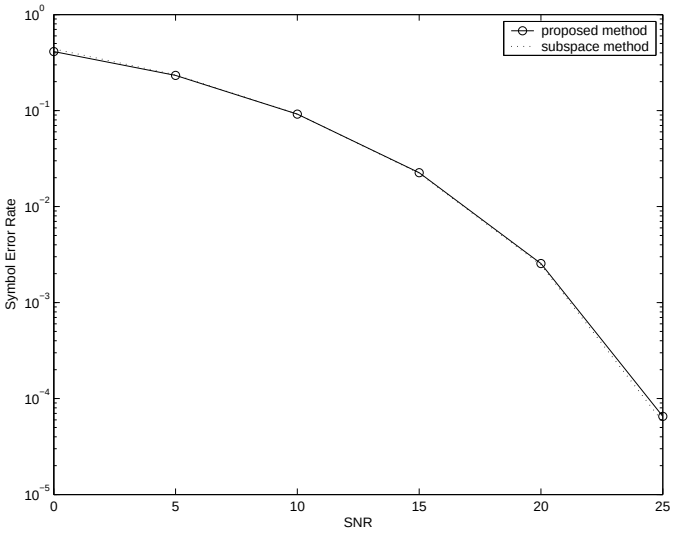

Figure 4.8. An OFDM system: symbol error rate versus output SNR

Chapter 5

Conclusions

We develop three blind identification algorithms for MIMO frequency selective wireless communication channels. Instead of computing the channel matrix directly from the covariance matrix of the received data, as in subspace methods, the algorithms compute the channel product matrixes first and then determine the channel impulse response matrix via an eigenvalue-eigenvector decomposition. The algorithms are simple, in terms of the amount of computations required, as compared with subspace methods; they allow a more relaxed identifiability condition and are applicable to MIMO systems with more transmitters or more receivers. Simulation results show that they are reasonably robust with respect to channel order overestimation and has an NRMSE performance comparable to subspace methods.

The algorithms differ in precoding complexity. The three precoding considered are: (i) periodic precoding, (ii) periodic precoding plus zero padding, and (iii) zero padding alone. As a result, for each of the three cases, the computation required to determine the channel product matrices are also different. The computations required are respectively (i) to solve a decoupled group of overdetermined linear systems of equations, (ii) to solve a triangular linear system, and (iii) to carry out a number of simple subtractions. The simplified computation in (iii) comes at the price of about 3 dB increase in NRMSE as compared to (i) and (ii).

Appendix

A Proof of Proposition 4.1 and 4.2

Preliminary :

For each j, let $\mathbf{N}_j \in \mathbb{R}^{(N-j)\times(L-j+1)}$ be similarly defined as (2.17), except that $\mathbf{I}_{M_r}$ is replaced by 1. It can be easily check that there exists permutation matrices $\mathbf{P}_{\mathbf{l_j}} \in \mathbb{R}^{M_r(N-j)\times M_r(N-j)}$ and $\mathbf{P}_{\mathbf{r_j}} \in \mathbb{R}^{M_r(L-j+1)\times M_r(L-j+1)}$ such that $\mathbf{P}_{\mathbf{l_j}}\mathbf{M}_j\mathbf{P}_{\mathbf{r_j}} = \mathrm{diag}[\mathbf{N}_j, \mathbf{N}_j, \cdots, \mathbf{N}_j] = \mathbf{D}_j \in \mathbb{R}^{M_r(N-j)\times M_r(L-j+1)}$ is a block diagonal matrix with each block of dimension $(N-j)\times(L-j+1)$. Since ${\mathbf{P}_{\mathbf{l_j}}}^T = {\mathbf{P}_{\mathbf{l_j}}}^{-1}$ and ${\mathbf{P}_{\mathbf{r_j}}}^T = {\mathbf{P}_{\mathbf{r_j}}}^{-1}$ [34, p.110], we have $\mathbf{M}_j = {\mathbf{P}_{\mathbf{l_j}}}^T\mathbf{D}_j{\mathbf{P}_{\mathbf{r_j}}}^T$. Hence $\mathbf{M}_j$ is full column rank if and only if $\mathbf{N}_j$ is full column rank for $j = 0, 1, \cdots, L$.

Also, $\mathbf{M}_j^T\mathbf{M}_j = (\mathbf{P}_{\mathbf{r_j}}\mathbf{D}_j^T\mathbf{P}_{\mathbf{l_j}})({\mathbf{P}_{\mathbf{l_j}}}^T\mathbf{D}_j{\mathbf{P}_{\mathbf{r_j}}}^T) = \mathbf{P}_{\mathbf{r_j}}\mathbf{D}_j^T\mathbf{D}_j{\mathbf{P}_{\mathbf{r_j}}}^T = \mathbf{P}_{\mathbf{r_j}}\mathrm{diag}[\mathbf{N}_j^T\mathbf{N}_j, \cdots, \mathbf{N}_j^T\mathbf{N}_j]{\mathbf{P}_{\mathbf{r_j}}}^T$. Let $\lambda(\mathbf{A})$ denote the spectrum of $\mathbf{A}$ [34, p.310], that is, the set of eigenvalues of $\mathbf{A}$. Then $\lambda(\mathbf{M}_j^T\mathbf{M}_j) = \lambda(\mathbf{N}_j^T\mathbf{N}_j)$.

Proof of Proposition 2.2 :

If at $N - L + 1 \le m \le N - 2$, it can be checked that $\mathbf{N}_j$, $j = 2, 3, \cdots, L-1$ is not of full column rank since it has two columns both equal to $[\tau\ \tau \cdots \tau]^T$ which implies that at least one $\mathbf{M}_j$ is rank deficient and vice versa.

Proof of Proposition 2.3 :

From the **Preliminary**, since $\lambda(\mathbf{M}_j^T\mathbf{M}_j) = \lambda(\mathbf{N}_j^T\mathbf{N}_j)$, the condition number of $\mathbf{M}_j^T\mathbf{M}_j$ is identical to that of $\mathbf{N}_j^T\mathbf{N}_j$, i.e., $\kappa(\mathbf{M}_j^T\mathbf{M}_j) = \kappa(\mathbf{N}_j^T\mathbf{N}_j)$. Thus we need only compute the condition number of $\mathbf{N}_j^T\mathbf{N}_j$.

Case (a): For $m = 0, m = 1, \cdots$, and $m = N - L - 1$, we know

$$\mathbf{N}_j^T\mathbf{N}_j = a \cdot \mathbf{I}_{L-j+1} + (2b + c_j) \cdot [1 \cdots 1]^T[1 \cdots 1], \tag{A.1}$$

where $a = N^2(1-\tau)^2$, $b = N\tau(1-\tau)$, $c_j = (N-j)\tau^2$. Hence the maximum and minimum

eigenvalues are $a+(L-j+1)(2b+c_j)$ and a respectively. Thus the condition number of $\mathbf{M}_j^T\mathbf{M}_j$ is $1+[(L-j+1)(2b+c_j)/a]$ which is a decreasing function of j. Therefore the corresponding μ is equal to $\mu_1 = 1+[(L+1)(2b+c_0)/a]$.

Case (b): For $m = N-L$ and $m = N-1$, we consider the $j=0$ case and $j \neq 0$ case for N_j separately. For $j=0$ with $m = N-L$ or $m = N-1$, direct multiplication of $\mathbf{N}_0^T\mathbf{N}_0$ gives the same matrix as (A.1), and the condition number of $\mathbf{M}_0^T\mathbf{M}_0$ is μ_1. For $j \neq 0$ with $m = N-L$, direct multiplication of $\mathbf{N}_j^T\mathbf{N}_j$ yields

$$\mathbf{N}_j^T\mathbf{N}_j = \begin{bmatrix} a+2b+c_j & 2b+c_j & 2b+c_j & \cdots & 2b+c_j & b+c_j \\ 2b+c_j & a+2b+c_j & 2b+c_j & \cdots & 2b+c_j & b+c_j \\ \vdots & \vdots & \ddots & \vdots & \vdots & \vdots \\ 2b+c_j & 2b+c_j & 2b+c_j & \cdots & a+2b+c_j & b+c_j \\ b+c_j & b+c_j & b+c_j & \cdots & b+c_j & c_j \end{bmatrix} \in \mathbb{R}^{(L-j+1)\times(L-j+1)}. \tag{A.2}$$

The eigenvalues of $\mathbf{N}_j^T\mathbf{N}_j$ in ascending order, are α_j, a, β_j, where a has a multiplicity $L-j-1$, and $\beta_j = \frac{1}{2}\{(L-j)(2b+c_j)+(a+c_j)+\sqrt{[(L-j)(2b+c_j)+(a-c_j)]^2+4(L-j)(b+c_j)^2}\}$, $\alpha_j = \frac{1}{2}\{(L-j)(2b+c_j)+(a+c_j)-\sqrt{[(L-j)(2b+c_j)+(a-c_j)]^2+4(L-j)(b+c_j)^2}\}$. All of the eigenvalues are positive and real. (A proof is given in Appendix B). It can be similarly shown that for $j \neq 0$ with $m = N-1$, $\mathbf{N}_j^T\mathbf{N}_j$ has the same eigenvalues α_j, a, β_j. Hence for $j = 1, 2, \cdots, L$, $\lambda(\mathbf{M}_j^T\mathbf{M}_j) = \{\alpha_j, a, \beta_j\}$ and the condition number is

$$\kappa(\mathbf{M}_j^T\mathbf{M}_j) = \frac{\beta_j}{\alpha_j} = 1 + \frac{\chi_j^2 - 4(N-L)b^2 + \chi_j\sqrt{\chi_j^2 - 4(N-L)b^2}}{2(N-L)b^2}, \tag{A.3}$$

where $\chi_j = (L-j)(2b+c_j)+a+c_j$. Since β_j/α_j is also a decreasing function of j, then the maximum value is β_1/α_1. Therefore, combining the two cases ($j=0, j\neq 0$), the corresponding μ is $\mu_2 = \max\{\mu_1, \beta_1/\alpha_1\} \geq \mu_1$.

B The Eigenvalues of $\mathbf{N}_j^T\mathbf{N}_j$ for $m = N - L$

Proof :

Let $\mathbf{A}_j = \mathbf{N}_j^T\mathbf{N}_j$ defined in (A.2), then $\mathbf{A}_j$ is positive definite since $\mathbf{N}_j$ is full column rank. It can be checked that the eigenvectors corresponding to $(L-j-1)$ multiple eigenvalue a are: $[1,-1,0,0,\cdots,0]^T$, $[1,1,-2,0,\cdots,0]^T$, $\cdots$, $[1,1,\cdots,1,-(L-j-1),0]^T$. The remaining eigenvectors are $[1,1,\cdots,1,x]^T \in \mathbb{R}^{L-j+1}$. Hence

$$\mathbf{A}_j \begin{bmatrix} 1 \\ \vdots \\ 1 \\ x \end{bmatrix} = \begin{bmatrix} a+(L-j)(2b+c_j)+(b+c_j)x \\ \vdots \\ a+(L-j)(2b+c_j)+(b+c_j)x \\ (L-j)(b+c_j)+c_jx \end{bmatrix} = \lambda_j \begin{bmatrix} 1 \\ \vdots \\ 1 \\ x \end{bmatrix}, \tag{B.1}$$

which implies the following two equations

$$a+(L-j)(2b+c_j)+(b+c_j)x = \lambda_j, \tag{B.2}$$

$$(L-j)(b+c_j)+c_jx = \lambda_j x. \tag{B.3}$$

Substitute (B.2) into (B.3), we can get an second order equation of x. Solving this equation can lead to two solutions of x. Bring these two x into (B.2) and we can obtain the two eigenvalues β_j, α_j. In addition, $\beta_j \geq a$ because of (B.4)

$$\begin{aligned} \beta_j &= \tfrac{1}{2}\{(L-j)(2b+c_j)+(a+c_j)+\sqrt{[(L-j)(2b+c_j)+a-c_j]^2+4(L-j)(b+c_j)^2}\} \\ &\geq \tfrac{1}{2}\{(L-j)(2b+c_j)+(a+c_j)+\sqrt{[(L-j)(2b+c_j)+a-c_j]^2}\} \\ &= \tfrac{1}{2}\{[(L-j)(2b+c_j)+(a+c_j)+[(L-j)(2b+c_j)+a-c_j]\} \\ &= a+(L-j)(2b+c_j) \\ &\geq a \end{aligned} \tag{B.4}$$

and $\alpha_j \leq a$ because of the interlacing property [34, p.396].

C A Proof of $\frac{\partial f(\alpha,\beta)}{\partial \alpha} > 0$

With $f(\alpha,\beta) = \frac{(\alpha+1)^{2(L+1)}+2(L+1)(\alpha+2)-1}{\beta^2(\alpha+2)^2}$ for $\alpha > 0$, $L \geq 1$,

$$
\begin{aligned}
\tfrac{\partial f(\alpha,\beta)}{\partial \alpha} &= \tfrac{1}{\beta^2}\{(\alpha+2)^{-2}[2(L+1)(\alpha+1)^{2L+1}+2(L+1)] - 2(\alpha+2)^{-3}[(\alpha+1)^{2(L+1)}+2(L+1)(\alpha+2)-1]\} \\
&= \tfrac{1}{\beta^2(\alpha+2)^3}[2(L+1)(\alpha+1)^{2L+1}(\alpha+1+1)+2(L+1)(\alpha+2)-2(\alpha+1)^{2(L+1)}-4(L+1)(\alpha+2)+2] \\
&= \tfrac{1}{\beta^2(\alpha+2)^3}[2(L+1)(\alpha+1)^{2(L+1)}+2(L+1)(\alpha+1)^{2L+1}-2(L+1)(\alpha+2)-2(\alpha+1)^{2(L+1)}+2] \\
&= \tfrac{1}{\beta^2(\alpha+2)^3}[2L(\alpha+1)^{2(L+1)}+2(L+1)(\alpha+1)^{2L+1}-2(L+1)(\alpha+2)+2] \\
&\geq \tfrac{1}{\beta^2(\alpha+2)^3}[2L(\alpha+1)^{2(L+1)}+2(L+1)(\alpha+1)^{3}-2(L+1)(\alpha+2)+2] \\
&= \tfrac{1}{\beta^2(\alpha+2)^3}[2L(\alpha+1)^{2(L+1)}-2L+4L\alpha+4\alpha+2L\alpha^3+6L\alpha^2+2\alpha^3+6\alpha^2] \\
&= \tfrac{1}{\beta^2(\alpha+2)^3}\{2L[(\alpha+1)^{2(L+1)}-1]+4L\alpha+4\alpha+2L\alpha^3+6L\alpha^2+2\alpha^3+6\alpha^2\} \\
&> 0.
\end{aligned}
$$

D A Proof of Proposition 3.1

Let $a = L + 1 - L\tau$ and $b = \tau$, then according to (3.27), $\bar{g}_0 = \frac{1}{a} > 0$ and $\bar{g}_i = -\frac{b}{a^2}(1-\frac{b}{a})^{i-1} < 0$ for $i = 1, 2, \cdots, L$, and

$$\begin{aligned}
\bar{g}_0 + \bar{g}_1 + \bar{g}_2 + \cdots + \bar{g}_l &= \tfrac{1}{a} - \tfrac{b}{a^2} - \tfrac{b}{a^2}(1-\tfrac{b}{a}) - \cdots - \tfrac{b}{a^2}(1-\tfrac{b}{a})^{l-1} \\
&= \tfrac{1}{a} - \tfrac{b}{a^2} \cdot \tfrac{1\cdot[1-(1-\frac{b}{a})^l]}{1-(1-\frac{b}{a})} \\
&= \tfrac{1}{a} - \tfrac{1}{a}[1-(1-\tfrac{b}{a})^l] \\
&= \tfrac{1}{a}(1-\tfrac{b}{a})^l
\end{aligned}$$

Hence

$$\begin{aligned}
\|\mathbf{m}\|_2^2 &= \bar{g}_0^2 + (\bar{g}_0+\bar{g}_1)^2 + \cdots + (\bar{g}_0+\bar{g}_1+\cdots+\bar{g}_L)^2 \\
&= [\tfrac{1}{a}]^2 + [\tfrac{1}{a}(1-\tfrac{b}{a})]^2 + \cdots + [\tfrac{1}{a}(1-\tfrac{b}{a})^L]^2 \\
&= \tfrac{1}{a^2}[1 + (1-\tfrac{b}{a})^2 + \cdots + (1-\tfrac{b}{a})^{2L}] \\
&= \tfrac{1}{a^2} \cdot \tfrac{1\cdot[1-(1-\frac{b}{a})^{2(L+1)}]}{1-(1-\frac{b}{a})^2} \\
&= \tfrac{1-(1-\frac{b}{a})^{2(L+1)}}{a^2\cdot[1-1-\frac{b^2}{a^2}+\frac{2b}{a}]} \\
&= \tfrac{1-(1-\frac{b}{a})^{2(L+1)}}{2ab-b^2} \\
&= \tfrac{1-(1-\frac{\tau}{L+1-L\tau})^{2(L+1)}}{2(L+1-L\tau)\tau-\tau^2}
\end{aligned}$$

and

$$\begin{aligned}
\tfrac{d}{d\tau}\|\mathbf{m}\|_2^2 &= \tfrac{[2(L+1-L\tau)\tau-\tau^2]\cdot[-2(L+1)(1-\frac{\tau}{L+1-L\tau})^{2L+1}]\cdot[-\frac{d}{d\tau}(\frac{\tau}{L+1-L\tau})]}{[2(L+1-L\tau)\tau-\tau^2]^2} - \tfrac{[1-(1-\frac{\tau}{L+1-L\tau})^{2(L+1)}]\cdot(-4L\tau-2\tau)}{[2(L+1-L\tau)\tau-\tau^2]^2} \\
&= \tfrac{[(1-\tau)\tau(2L+1)+\tau]\cdot[2(L+1)(1-\frac{\tau}{L+1-L\tau})^{2L+1}]\cdot[\frac{L+1}{(L+1-L\tau)^2}]}{[2(L+1-L\tau)\tau-\tau^2]^2} + \tfrac{[1-(1-\frac{\tau}{L+1-L\tau})^{2(L+1)}]\cdot(4L\tau+2\tau)}{[2(L+1-L\tau)\tau-\tau^2]^2}
\end{aligned}$$

Because $0 < 1-\tau < 1$ and $0 < (1-\frac{\tau}{L+1-L\tau}) < 1$ for $0 < \tau < 1$, $\frac{d}{d\tau}\|\mathbf{m}\|_2^2 > 0$ for $0 < \tau < 1$.

Bibliography

[1] Z. Ding and Y. Li, *Blind Equalization and Identification*, Marcel Dekker, Inc., 2001.

[2] G. B. Giannakis, Y. Hua, P. Stoica, and L. Tong, *Signal Processing Advances in Wireless and Mobile Communications Volume I: Trends in Channel Identification and Equalization*, Prentice Hall PTR, 2001.

[3] J. K. Tugnait, "Blind spatio-temporal equalization and impulse response estimation for MIMO channels using a Godard cost function", *IEEE Trans. Signal Processing*, vol. 45, no. 1, pp. 268-271, Jan 1997.

[4] A.J. van der Veen, S. Talwar, and A. Paulraj, "Blind estimation of multiple digital signals transmitted over FIR channels", *IEEE Signal Processing Letters*, vol. 2, no. 5, pp. 99-102, May 1995.

[5] J. Liang and Z. Ding, "Blind MIMO system identification based on cumulant subspace decomposition", *IEEE Trans. Signal Processing*, vol. 51, no. 6, pp. 1457-1468, June 2003.

[6] A.J. van der Veen, S. Talwar, and A. Paulraj, "A subspace approach to blind space-time signal processing for wireless communication systems", *IEEE Trans. Signal Processing*, vol. 45, no. 1, pp. 173-190, Jan. 1997.

[7] H. Liu and G. Xu, "Closed-form blind symbol estimation in digital communications", *IEEE Trans. Signal Processing*, vol. 43, no. 11, pp. 2714-2723, Nov. 1995.

[8] Y. Hua, K. Abed-Meraim, and M. Wax, "Blind system identification using minimum noise subspace", *IEEE Trans. Signal Processing*, vol. 45, no. 3, pp. 770-773, March 1997.

[9] A. Gorokhov and P. Loubation, "Subspace-based techniques for blind separation of convolutive mixtures with temporally correlated sources", *IEEE Trans. Circuit and Systems, Part I*, vol. 44, no. 9, pp. 813-820, Sep. 1997.

[10] A. Gorokhov and P. Loubation, "Blind identification of MIMO-FIR systems: a generalized linear prediction approach", *Signal Processing*, vol. 73, pp. 105-124, 1999.

[11] J. K. Tugnait, "On linear predictors for MIMO channels and related blind identification and equalization", *IEEE Signal Processing Letters*, vol. 5, no. 11, pp. 289-291, Nov. 1998.

[12] J. K. Tugnait and B. Huang "Multistep linear predictors-based blind identification and equalization of multiple-input multiple-output channels", *IEEE Trans. Signal Processing*, vol. 48, no. 1, pp. 26-38, Jan 2000.

[13] A. Scaglione, G. B. Giannakis, and S. Barbarossa, "Redundant filter bank precoders and equalizers Part I: Unification and optimal designs.", *IEEE Trans. Signal Processing*, vol. 47, no. 7, pp. 1988-2006, July 1999.

[14] A. Scaglione, G. B. Giannakis, and S. Barbarossa, "Redundant filter bank precoders and equalizers Part II: Blind channel estimation, synchronization, and direct equalization", *IEEE Trans. Signal Processing*, vol. 47, no. 7, pp. 2007-2022, July 1999.

[15] A. Chevreuil, E. Serpedin, P. Loubaton and G. B. Giannakis, "Blind channel identification and equalization using periodic modulation precoders: performanve analysis", *IEEE Trans. Signal Processing*, vol. 48, no. 6, pp. 1570-1586, June 2000.

[16] C. A. Lin and J. W. Wu, "Blind identification with periodic modulation: A time-domain approach", *IEEE Trans. Signal Processing*, vol. 50, no. 11 pp. 2875-2888, Nov. 2002.

[17] A. Chevreuil and P. Loubaton, "MIMO blind second-order equalization method and conjugate cyclostationarity", *IEEE Trans. Signal Processing*, vol. 47, no. 2, pp. 572-578, Feb. 1999.

[18] H. Bölcskei, R. W. Heath, Jr., and A. J. Paulraj, "Blind channel estimation in spatial multiplexing systems using nonredundant antenna precoding", *Proc. of the 33rd Annual IEEE Asilomar Conf. on Signals, Systems, and Computers*, vol. 2, pp. 1127-1132, Oct. 1999.

[19] H. Bölcskei, R. W. Heath, Jr., and A. J. Paulraj, "Blind channel identification and equalization in OFDM-based multiantenna systems", *IEEE Trans. Signal Processing*, vol. 50, no. 1, pp. 96-109, Jan. 2002.

[20] Z. Ding, "Matrix outer-product decomposition method for blind multiple channel identification", *IEEE Trans. Signal Processing*, vol. 45, no. 12, pp. 3053-3061, Dec. 1997.

[21] Z. Ding and L. Qiu, "Blind MIMO channel identification from second order statistics using rank deficient channel convolution matrix", *IEEE Trans. Signal Processing*, vol. 51, no. 2, pp. 535-544, Feb. 2003.

[22] J. Shen and Z. Ding, "Direct blind MMSE channel equalization based on second-order statistics", *IEEE Trans. Signal Processing*, vol. 48, no. 4, pp. 1015-1022, April 2000.

[23] Z. Ding and D. B. Ward, "Subspace approach to blind and semi-blind channel estimation for space-time block codes", *IEEE Trans. Wireless Communications*, vol. 4, no. 2, pp. 357-362, March 2005.

[24] E. Moulines, P. Duhamel, J-F. Cardoso, and S. Mayrargue, "Subspace method for the blind identification of multichannel FIR filters", *IEEE Trans. Signal Processing*, vol. 43, no. 2, pp. 516-525, Feb. 1995.

[25] Z. Wang, X. Ma, and G. B. Giannakis, "Optimality of single-carrier zero-padding block transmission", *in Proc. Wireless Communications and Networking Conference*, vol. 2, pp. 660-664, March 2002.

[26] Y. H. Zeng and T. S. Ng, "A semi-blind channel estimation method for multiuser multiantenna OFDM systems", *IEEE Trans. Signal Processing*, vol. 52, no. 5, pp. 1419-1429, May 2004.

[27] J. Y. Wu and T. S. Lee, "Periodic-modulation-based blind channel identification for the single-carrier block transmission with frequency-domain equalization", *IEEE Trans. on Signal Processing*, vol. 54, no. 3, pp.1114-1130, March, 2006.

[28] W. Hachem, F. Desbouvries, and P. Loubaton, "MIMO channel blind identification in the presence of spatially correlated noise", *IEEE Trans. Signal Processing*, vol. 50, no. 3, pp. 651-661, March 2002.

[29] Y. H. Zeng and T. S. Ng, "A blind MIMO channel estimation method robust to order overestimation", *Signal Processing*, vol. 84, pp. 435-439, 2004.

[30] R. E. Bach, JR. and Y. Baram, "Recursive inversion of externally defined linear systems by FIR filters", *IEEE Trans. Automatic Control*, vol. 34, no. 6, pp. 635-637, June 1989.

[31] D. Commenges and M. Monsion, "Fast inversion of triangular Toeplitz matrices", *IEEE Trans. Automatic Control*, vol. 29, no. 3, pp. 250-251, March 1984.

[32] N. J. Higham, "A survey of condition number estimation for triangular matrices", *SIAM Review*, vol. 29, no. 4, pp. 575-596, Dec 1987.

[33] M. W. Hirsch and S. Smale, *Differential Equations, Dynamical Systems, and Linear Algebra*, Academic Press, 1974.

[34] G. H. Golub and C. F. Van Loan, *Matrix Computions*, 3rd edition, The Johns Hopkins University Press, 1996.

[35] F. Zhang, *Matrix Theory: Basic Results and Techniques*, Springer-Verlag , 1999.

[36] B. O'Hara and A. Petrick, *The IEEE 802.11 Handbook: A Designer's Companion*, 2nd edition, 2nd edition, IEEE Press, 2005.

[37] P. Lancaster and M. Tismenetsky, *The Theory of Matrices With Applications*, Academic Press, 1984.

[38] D. G. Luenberger, *Linear and Nonlinear Programming*, 2nd edition, Kluwer Academic Publishers, 2003.

A List of Publications in Conferences and Journals

[**1**] C. A. Lin and Y. S. Chen, "Blind identification of MIMO channels using optimal periodic precoding" accepted for publication in *IEEE trans. on Circuits and Systems I: Fundamental Theory and Applications*. (Part of this work was presented in IEEE international Symposium on Circuits and Systems, Kobe, Japan, May 2005.)

[**2**] Y. S. Chen and C. A. Lin, "Blind identification of MIMO channels in zero padding block transmission systems" accepted for publication in *IEEE trans. on Signal Processing*. (Part of this work was presented in CACS Automatic Control Conference, Tainan, Taiwan, Nov. 2005.)

[**3**] Y. S. Chen and C. A. Lin, "Blind channel identification for MIMO single carrier zero padding block transmission systems" submitted to *IEEE trans. on Signal Processing*. (Part of this work was presented in IEEE Workshop on Signal Processing Advances in Wireless Communications, Cannes, France, July 2006.)